Chapter 5
Conjugated Polymer Photovoltaic Materials

Long Ye and Jianhui Hou

5.1 Introduction

During the past few decades, conjugated polymers with various molecular structures have been explored for applications in polymer solar cells (PSCs). In order to obtain more efficient PSCs, great effort has been devoted to optimizing and synthesizing conjugated polymers with superior photovoltaic properties, which boost the power conversion efficiency (*PCE*) toward or even above 8–10 % in several research groups [1–13]. In this chapter, an overview of conjugated polymer photovoltaic materials is given to provide insights for molecular design and fine-tuning of high-performance photovoltaic polymers. First, we briefly summarize and provide design considerations of conjugated polymer photovoltaic materials. Second, representative photovoltaic polymers are introduced. Third, representative conjugated polymer acceptor materials are briefly introduced and discussed. Because photovoltaic properties of conjugated polymers are susceptible to device fabrication conditions and device structures, excluding the factors of optical and interfacial enhancement by device engineering, the '*initial PCE*' of the PSCs used in simple conventional devices of ITO/PEDOT: PSS/Polymer: PCBM/Ca (or Mg, Ba, LiF)/Al (or Ag, Au), as depicted in Fig. 5.1, is discussed.

L. Ye · J. Hou (✉)
State Key Laboratory of Polymer Physics and Chemistry, Beijing National Laboratory for Molecular Sciences, Institute of Chemistry, Chinese Academy of Sciences, Beijing 100190, People's Republic of China
e-mail: hjhzlz@iccas.ac.cn

Y. Li (ed.), *Organic Optoelectronic Materials*,
Lecture Notes in Chemistry 91, DOI 10.1007/978-3-319-16862-3_5

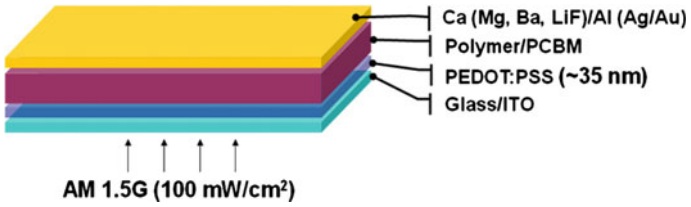

Fig. 5.1 Simple conventional device structure of a polymer solar cell

5.1.1 Brief Summary of Photovoltaic Polymers

As the key photovoltaic materials in PSCs, conjugated polymers can be classified into two types, namely donor and acceptor photovoltaic polymers. Following the pioneering works of Heeger et al. and Friend et al. in the 1990s [14, 15], thousands of polymer donors with different backbones and side groups have been developed, synthesized, and used in polymer solar cells during the past few decades, and have been deemed to be one of the driving forces of the development of PSCs. Conjugated polymer photovoltaic donor materials have been well discussed and reviewed recently [16–30]. However, to classify the polymer donors rationally is still quite difficult because of the rapid growth of the numbers of polymer donors. Herein, three types of the first used homopolymer donor materials, i.e., the derivatives of poly(1,4-phenylene vinylene) (PPVs), polythiophene (PTs), poly(thienylene vinylene) (PTVs), etc., are discussed as the first category of polymer donors (see Fig. 5.2). In recent years, the Donor–Acceptor copolymers (D–A copolymers) based on two or more conjugated building blocks have played important roles in promoting the development of the PSC field, so we provide more examples of conjugated D–A copolymers as the second category of polymer donors. For example, benzothiadiazole (BT)-based polymers, silole-containing polymers, diketopyrrolopyrrole (DPP)-based polymers, indacenodithiophene (IDT)-based polymers, Benzo[1,2-b:4,5-b′]dithiophene (BDT) based polymers, Thienopyrroledione (TPD) based polymers, etc., are introduced and discussed (see Fig. 5.2). In comparison with polymer donors, polymer acceptors have attracted less attention, although some recent work has shown that polymer acceptors have great potential in realizing highly efficient PSCs without using fullerene derivatives. Therefore, in the last section of this chapter, we give a brief introduction of polymer acceptors.

5.1.2 Design Considerations of Conjugated Polymer Photovoltaic Materials

The basic requirements for molecular design of high efficiency photovoltaic polymers have been discussed and summarized in several reviews [16–25]. It is known

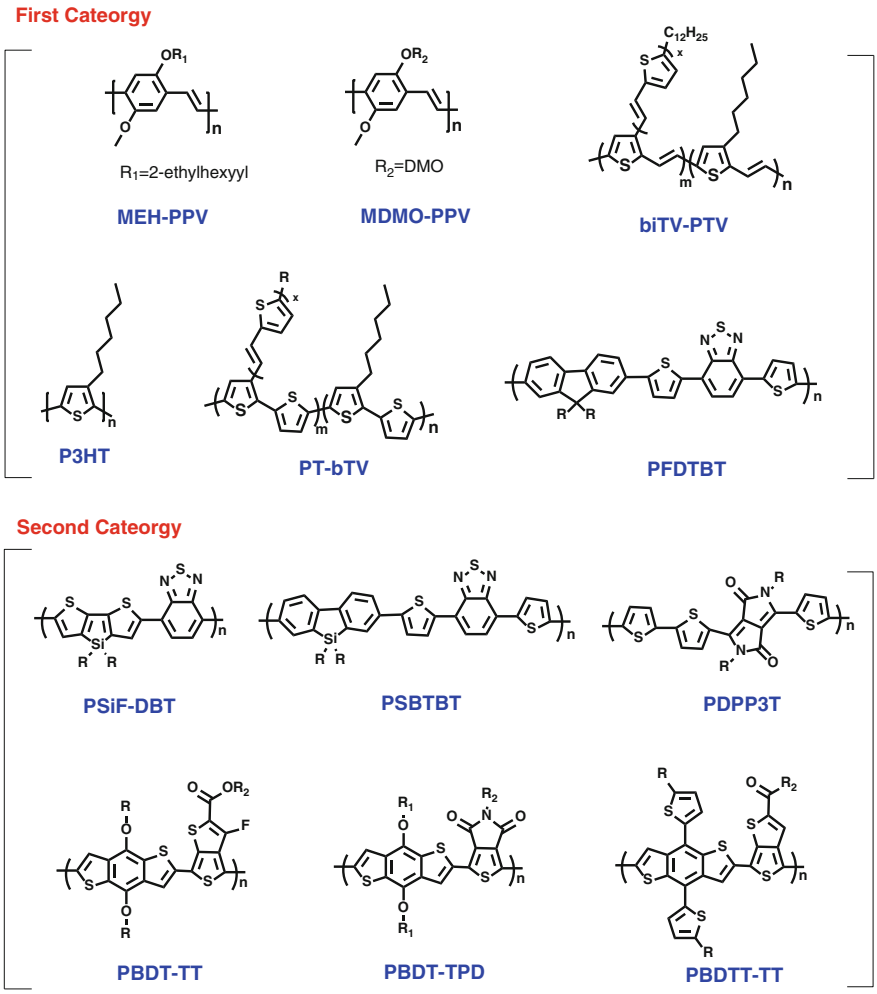

Fig. 5.2 Two categories of polymer donor materials and examples of representative polymers in each category

that the *PCE* of PSC can be calculated based on three photovoltaic parameters: the open circuit voltage (V_{oc}), the short circuit current (J_{sc}), and the fill factor (*FF*). For highly efficient photovoltaic polymers, important factors including solubility, light absorption, molecular energy level, mobility as well as morphology should be considered.

Appropriate solubility and good film-forming properties should first be considered in designing novel conjugated polymers. To get high quality thin films of conjugated polymers by solution coating processes, conjugated polymer donor materials must have good solubility in commonly used organic solvents such as

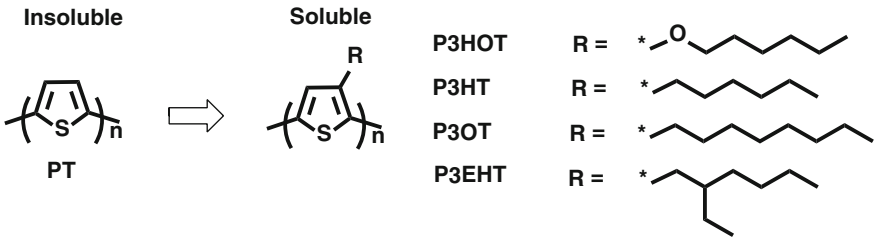

Fig. 5.3 Unsubstituted and substituted PTs

chloroform (CF), chlorobenzene (CB), toluene, and dichlorobenzene (DCB). Because conjugated polymers have rigid backbones and intermolecular π–π interaction provides strong driving force for aggregation, the unsubstituted conjugated polymers are all insoluble in organic solvents. Therefore, long, flexible and/or branched side groups, such as alkyls or alkoxys, are introduced as functional groups onto their backbones to overcome the strong aggregation effect and hence to afford solution processability for conjugated polymers. For example, as shown in Fig. 5.3, the unsubstituted polythiophene is an insoluble polymer; however, when alkyls, such as hexyl, octyl, or alkyls with more carbon numbers, are introduced as side groups, the derivatives can be readily dissolved in many types of organic solvents such as CF, toluene, CB, *o*-DCB, and so on.

For a polymer photovoltaic material, a broader and stronger absorption, matching well with the solar radiation spectrum, is necessary to achieve high J_{sc}. As shown in Fig. 5.4a, solar irradiation has a very broad spectrum, which is mainly distributed at the visible and infrared regions with a peak at ca. 700 nm, so to harvest solar light the photovoltaic polymer should absorb the majority of the wavelength region from 400 to 900 nm. Clearly, from the point of view of the absorption spectrum, the PSCs based on P3HT cannot make good use of solar light. Therefore, conjugated polymers with low band gaps (LBG polymers) were developed and used in PSCs, leading to the possibility of realizing high J_{sc}. In fact, the

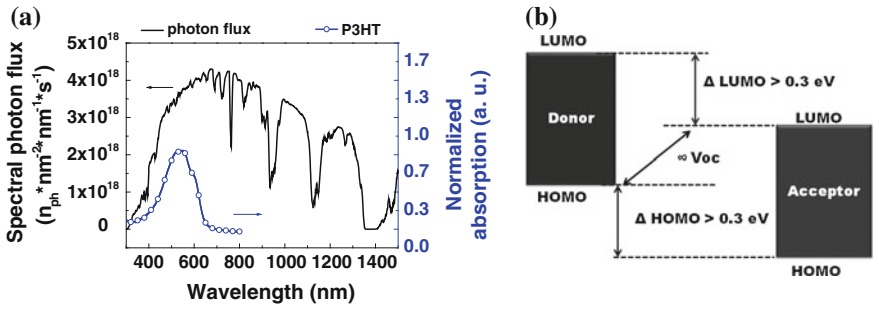

Fig. 5.4 **a** Spectral photon flux of AM 1.5 G and the UV-vis absorption of P3HT. **b** Schematic energy levels diagram of electron donors and acceptors in polymer solar cells

development of LBG polymers has played a very important role in the rapid progress in the PSC field.

The highest occupied molecular orbital (HOMO) and lowest unoccupied molecular orbital (LUMO) energy levels of photovoltaic polymers should be appropriate to maintain efficient charge separation and reduce energy loss. The schematic diagram of molecular energy and open-circuit voltage has been drawn in Fig. 5.4b. The value of V_{oc} for a PSC is directly proportional to the energy difference between the HOMO of the polymer donors and the LUMO of the acceptor materials [31]. As the LUMO of [6,6]-phenyl-C_{61} (or C_{71})-butyric acid methyl ester ($PC_{61}BM$ or $PC_{71}BM$) is generally considered to be −3.9 eV, the V_{oc} of polymer/PCBM-based polymer solar cells should rely on the HOMO level of polymers. Therefore, lowering the HOMO level of the polymer donors and thus reducing the energy loss during the charge separation process have been seen as key to achieving high V_{oc}.

Furthermore, in order to facilitate charge transport in the BHJ active layer, a high mobility should also be required for the polymer donors. The hole and electron mobility (μ_h and μ_e) are important parameters to evaluate the photovoltaic properties of the donor and acceptor photovoltaic materials. Moreover, in order to reduce or avoid germinate and bimolecular recombination in the BHJ layers, the donor and acceptor materials used in a BHJ active layer in a PSC device should have balanced mobilities for holes and electrons. For example, considering that μ_e of PCBM is ca. 10^{-3} $cm^2/(V\ s)$, when PCBM is used as the acceptor, μ_h of the polymer donors should be kept at the same level or higher than that of PCBM.

Morphological properties of polymer/PCBM blends are also of great importance for the photovoltaic performance of polymers [32–35]. For example, because of the low dielectric constants, the exciton diffusion length in the bulk of conjugated polymers is less than 10 nm, so nanoscale phase separation in the BHJ active layer is needed. If the aggregations of the donor and/or the acceptor are too big, the excitons are not diffused to the D/A interface efficiently, so that strong geminate recombination is observed. Besides of the size of phase separation in the BHJ blend, the crystallinity of conjugated polymers is also an important issue. As is well known, the transport of π-electrons in polymer aggregations is anisotropic, i.e., the intramolecular charge transport is along the conjugated backbones, whereas the intermolecular charge transport is along the overlapped π-orbits, which are perpendicular to the conjugated backbones. Therefore, various methods have been developed to modulate morphologies of conjugated polymers in the BHJ blends. For example, for the photovoltaic system based on a LBG polymer called PDPP3T [34] and PCBM, when the blend was processed with CF, a very low *PCE* (<2 %) was achieved; using CF and 1,8-diiodooctane as binary solvent, a moderate *PCE* of 4.7 % was achieved. Recently, Ye et al. [35] introduced a ternary solvent system of DCB/CF/DIO to optimize the morphology as well as the overall performance of the PDPP3T/PCBM system, which increased the *PCE* to 6.71 %. Morphological studies of the photovoltaic system of PDPP3T and PCBM clearly revealed that the phase separation size and the crystallinity of the polymer in the blend can be tuned effectively by modulating the processing solvents of the films. On the other hand,

morphologies of conjugated polymers can also be tuned by changing their molecular structures, which have been deemed as one of the main tasks for molecular design of conjugated polymers.

To meet the above requirements for highly efficient polymer donors, various molecular design strategies have been developed to modulate the photovoltaic properties of conjugated polymers and many new conjugated polymers have been designed and used in PSCs. In the following sections, the design strategies and some of the representative conjugated polymer photovoltaic materials are discussed in detail.

5.2 Conjugated Polymer Donor Materials

5.2.1 Three Important Types of Homopolymer

5.2.1.1 Poly(1,4-Phenylene Vinylene) Derivatives

In 1995, Yu et al. [14] pioneered the concept of the bulk-heterojunction (BHJ) in MEH-PPV:fullerene systems, which is considered to be the best PSC device architecture to date. Two poly(1,4-phenylene vinylene) (PPV) derivatives including poly [(2-methoxy-5-(2-ethyl-hexyloxy))-1,4-phenylenevinylene] MEH-PPV and poly[(2-methoxy-5-(3′,7′-dimethyloctyloxy))-1,4-phenylenevinylene] (MDMO-PPV) are very important donor polymers, which have played a very important role in the early stage of the development of the field of PSCs. Their molecular structure and corresponding photovoltaic results are shown in Fig. 5.5 and Table 5.1, respectively.

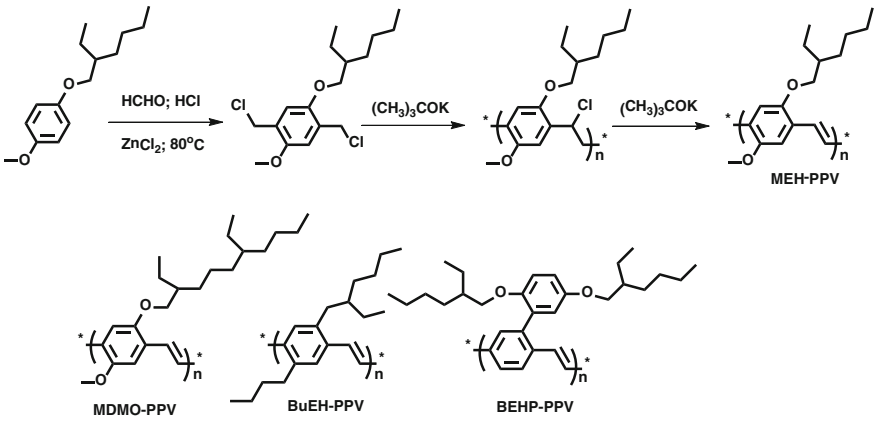

Fig. 5.5 Synthesis method and molecular structures of MEH-PPV and MDMO-PPV

Table 5.1 Photovoltaic results of some of the representative polymer donors of PPVs, PTVs, and the like

Materials	HOMO (eV)	V_{oc} (V)	J_{sc} (mA/cm^2)	FF (%)	PCE (%)	Ref.
MEH-PPV	−5.07	0.80	6.5	50	2.6	[42]
MDMO-PPV	−5.10	0.82	5.25	61	2.5	[40]
biTV-PTV	−4.77	0.48	2.27	30	0.32	[46]
P3CTV	−5.26	0.86	5.47	42.8	2.01	[47]
PBDTV	−5.16	0.71	6.46	57	2.63	[48]

MEH-PPV and MDMO-PPV show excellent solubility in commonly used solvents such as tetrahydrofuran, CF, toluene, xylenes, CB, and 1, 2-DCB. The solutions of these two polymers show very good film forming abilities, and the dilute solution of MEH-PPV or MDMO-PPV in CB (1–2 mg/mL) can still form high quality films by the spin coating process, which gives more opportunity to utilize these polymers to carry out studies in device physics and device engineering. Actually, these two polymers can also be used as electroluminescent materials in polymer light emitting devices.

PPV and its derivatives can be synthesized via various methods, including the Wessling precursor method [36], Gilch method [37], Heck coupling reaction [38], Knoevenagel polycondensation [39], etc. With the Wessling method, the PPV precursor can be synthesized by the reaction of bis-(sulfonium halide) salts of *p*-xylene with a base (NaOH) in water or alcohol solution, and then the precursor solution is spin-cast on ITO substrate, PPV film being formed by heat treatment at 180–300 °C under vacuum. The PPVs prepared by the Wessling precursor method have a lot of defects and impurities because of the oxidation of the precursor polymer, the residual precursor moieties, and undesired side reactions during the thermal conversion.

By Heck coupling reaction [38], organic halides and vinylbenzene compounds can be coupled to generate a carbon–carbon bond under the catalysis of Pd(0). Many functional groups, such as aldehyde, ester, nitryl, hydroxy and carboxy, have no obviously negative effects on the coupling reaction, so that this reaction has been widely used for preparation of PPVs. Cyano-substituted PPV can be readily prepared by the Knoevenagel polycondensation reaction between equimolar amounts of a terephthaldehyde derivative and a 1,4-diacetonnitrile-benzene derivative [39]. The condensation reaction takes place upon addition of excess potassium *tert*-butoxide or tetrabutylammonium hydroxide in THF/*tert*-butanol mixture at 50 °C. In the Knoevenagel condensation reaction, tetrabutylammonium hydroxide is used as catalyst, and the solvent for the reaction can be THF, toluene, or DMF.

As shown in Fig. 5.5, the Gilch method is very convenient to prepare PPV and its derivatives, and, by this method, 1,4-bis-chloromethyl-benzenes were treated with potassium *tert*-butoxide in non-hydroxylic solvents such as tetrahydrofuran [37]. The temperature of the reactant, the concentration of the monomer and the base, and the speed of the base addition are all crucial conditions for molecular

weight and PDI of the polymer. The molecular weight can also be controlled by using a benzylchloride derivative as the end capping reagent. Many PPV derivatives can be prepared with high molecular weight and high purity. Therefore, the Gilch method is the most successful method for the synthesis of PPVs, and the classic materials of PPVs, MEH-PPV and MDMO-PPV, are synthesized by this method.

A breakthrough in the *PCE* of the PSC devices based on PPV derivatives were presented by Brabec, Sariciftci, and coworkers [40]. In 2001, Shaheen et al. [40] introduced LiF as the *n*-type buffer layer in MDMO-PPV-based PSC devices and investigated the effect of processing solvent on the photovoltaic performance. By replacing toluene with CB, optimal phase separation and increased interactions between conjugated polymers were observed in MDMO-PPV-based PSC devices. As a result, a dramatically improved *PCE* up to 2.5 % was achieved, which was a nearly a threefold enhancement over previously reported values and also the world record at that time. Afterwards, Brabec et al. [41] systematically investigated the effect of the thickness of LiF on the photovoltaic performances of MDMO-PPV/$PC_{61}BM$-based PSC devices. Under optimal conditions, the PSC achieved an improved *PCE* of 3.3 %. Compared to PSCs without the LiF interfacial layer, the white light efficiencies of LiF-based PSC increased by over 20 %. Cao et al. [42] investigated the photovoltaic performance of MEH-PPV with a series of PCBM derivatives with different alkyl end groups on its side chain. The results revealed that the $PC_{61}BM$ derivative appending the butyl end group performs best as acceptor blended with MEH-PPV and achieved a high *PCE* of 2.6 %. Wienk et al. [43] incorporated $PC_{71}BM$ as the electron acceptor in thin-film polymer photovoltaic cells based on MDMO-PPV and provide a high J_{sc} because of the increased absorption in the visible region from $PC_{71}BM$ and an ultrafast charge transfer upon photoexcitation of MDMO-PPV or $PC_{71}BM$. In 2008, Tajima et al. [44] investigated the effect of regioregularity on the photovoltaic properties of the MDMO-PPV-based PSC devices. Fully regioregular MDMO-PPV was utilized for polymer photovoltaic devices, and their performance was compared with that of regiorandom MDMO-PPVs. A *PCE* up to 3.1 % was recorded in regioregular MDMO-PPV, whereas a moderate *PCE* of 1.7 % was achieved with regiorandom MDMO-PPV. The higher *PCE* of regioregular MDMO-PPV originated from both higher hole mobility and better nano-morphology. Mikroyannidis et al. [45] synthesized a novel LBG PPV derivative in 2010, which generated a record *PCE* for the PPV/PCBM system so far. However, although MEH-PPV and MDMO-PPV played vital roles in the early years (1995–2003) of PSC study, the narrow absorption range (400–560 nm) and poor hole mobility ($\sim 10^{-7}$ cm^2 V^{-1} s^{-1}) limited the photovoltaic performance of PPV derivatives.

5.2.1.2 Poly(thienylene vinylene) Derivatives and the Like

The likes of PPVs, poly(thienylene vinylene) derivatives (PTVs) were developed and applied in the PSC field because of their broad absorption and higher hole

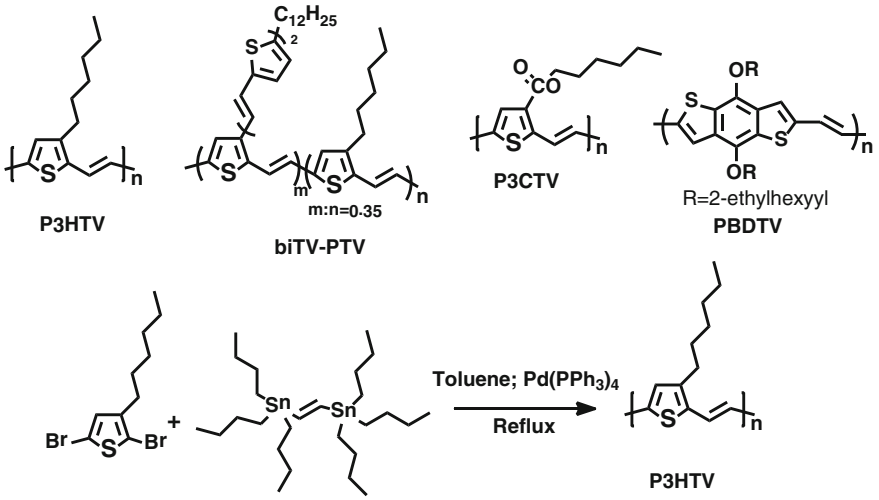

Fig. 5.6 Molecular structures and synthesis routes of PTVs

mobility. The molecular structure and corresponding photovoltaic results of a few PTV derivatives are provided in Fig. 5.6 and Table 5.1, respectively. Hexyl-substituted PTV, namely P3HTV, is the simplest soluble polymer among PTVs, although the photovoltaic performance of P3HTV is rather poor (PCE is ~0.2 %). The Stille coupling polycondensation reaction is widely used for synthesis of PTVs. As show in Fig. 5.6, PTVs can be easily prepared by using 2,5-dibromothiophenes and 1,2-bis-tributylstannylethylene as starting materials. In this reaction, aromatic solvents such as toluene, xylenes, and CB can be used as reaction solvents; the Pd(0) compound with appropriate ligand-like tetrakis(triphenylphosphine)palladium(0) can be used as the catalyst. Actually, the Stille coupling polycondensation reaction is also one of the most widely used methods for synthesis of other types of conjugated alternating copolymers. Therefore, although photovoltaic performance of the PSCs based on PTVs is quite low, the synthesis of PTVs paved the way for the study of molecular design and synthesis of highly efficient photovoltaic polymers.

Hou and Li et al. [46] introduced the conjugated side chains in the PTV backbone and synthesized a series of PTV derivatives with extended absorption in the UV-vis range from 350 to 740 nm. The *PCE* of the biTV-PTV-based PSC reached 0.32 %, which exhibited 52 % enhancement in comparison with that of the PSC device based on P3HTV under the same conditions. To overcome the intrinsic drawbacks of PTVs, for instance, high-lying HOMO levels and low V_{oc}, Li and coworkers [47] introduced an electron-deficient carboxylate group in P3HTV. The results indicated that the introduction of the carboxylate group in side chains can lower both LUMO and HOMO values of PTVs. Meanwhile, the photoluminescence of PTV can improved significantly. As a result, a higher V_{oc} up to 0.86 V was achieved. Under the D/A weight ratio of 1:2, a high *PCE* of 2.01 % was recorded. Notably, the *PCE* of the P3CTV-based PSC device is about 10 times higher than

that of the device based on P3HTV. The *PCE* of 2.01 % is the highest efficiency for PSCs based on PTVs. The dramatic improvement of the photovoltaic performances of PTV by the carboxylate substitution demonstrated that PTVs might be promising photovoltaic polymers upon suitable structural modification.

In 2010, He et al. [48] reported a new vinylene-based polymer, PBDTV, which was copolymerized by vinylene and BDT via Pd-catalyzed Stille-coupling method. The PBDTV film depicted a broad absorption range covering from 350 to 618 nm and high hole mobility of 4.84×10^{-3} cm^2 V^{-1} s^{-1}. At the optimal conditions (the weight ratio of PBDTV:$PC_{71}BM$ of 1:4 and the active layer thickness of 65 nm), the *PCE* of the PBDTV-based PSC device reached 2.63 % with V_{oc} of 0.71 V, J_{sc} of 6.46 mA/cm^2, and *FF* of 57 % under the illumination of AM 1.5G, 100 mW/cm^2.

5.2.1.3 Polythiophene Derivatives

Polythiophenes (PTs), particularly regioregular poly(3-alkylthiophene)s (P3ATs), are a widely used class of polymer donors because of their excellent thermal and chemical stability as well as good charge transport properties. The photovoltaic properties of representative polythiophene derivatives (see Fig. 5.7) are listed in Table 5.2. Because PTs do not dissolve in most of the common solvents, alkyl substitution is a useful method to help with the solubility of P3ATs. The length of alkyl group in P3ATs plays an important role in determining the solubility, crystallinity, and morphology.

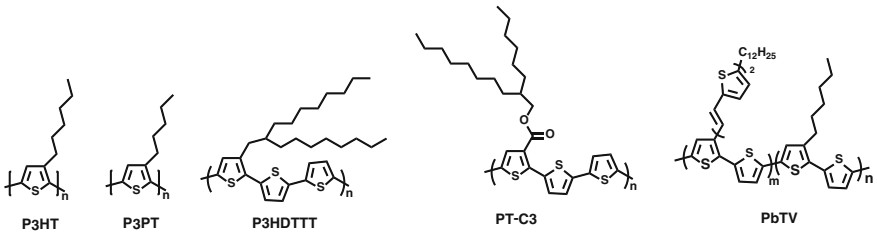

Fig. 5.7 Molecular structures of several PT derivatives

Table 5.2 Photovoltaic performances of some PT derivatives

Materials	HOMO (eV)	V_{oc} (V)	J_{sc} (mA/cm^2)	FF (%)	PCE (%)	Ref.
P3HT	−4.70	0.61	10.6	67.4	4.37	[61]
P3PT	−4.76	0.66	9.63	69	3.7	[69]
biTV-PT	−4.93	0.72	10.3	43	3.18	[73]
P3HDTTT	−5.30	0.82	6.33	66	3.4	[74]
PT-C3	−5.10	0.78	9.68	51.2	3.87	[75]

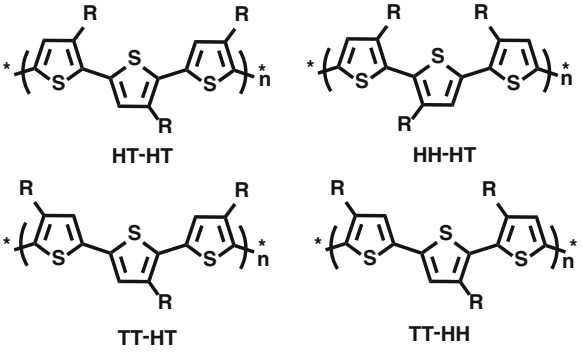

Fig. 5.8 Four regioisomers of poly(3-substituted thiophene)s

Generally, the polymerization of thiophenes is carried out at their 2- and 5-positions. For many PTs, such as poly(3-alkylthiophene)s, the repeated units are asymmetric, so there are three relative orientations available when two thiophene rings are coupled between the 2- and 5-positions. Usually, the 2-position is called the head, and the 5-position the tail. As shown in Fig. 5.8, this leads to a mixture of four regioisomers when 3-substituted (or asymmetric) thiophene monomers are employed [49]. The HT-HT structure of PTs is seen as regioregular polymers, and the HT-HT isomer proportion in the polymer is known as regioregularity. Regioregular poly(3-substituted thiophene) can easily access a low energy planar conformation, so the regioregularity is an important factor in characterization of poly(3-substituted thiophene).

^{1}H and ^{13}C NMR can be used to determine the structure and the regioregularity of PTs [50]. In a regioregular PT (HT-coupling ≈ 100 %), the proton at the 4-position of thiophene exhibits a neat peak at δ = 6.98. There are four chemically distinct triad regioisomers in regioirregular PATs, as shown in Fig. 5.9. In ^{1}H NMR spectra, the TT-HT isomer has a peak at δ = 7.00, HH-TT isomer has a peak at δ = 7.05, and the HT-HH isomer has a peak at δ = 7.02. Therefore, using the integral area of the peaks, the relative ratio of HT-HT couplings to non-HT-HT couplings can be determined. In the ^{13}C NMR spectrum, regioregular PTs exhibits four resonances in the aromatic region (δ = 128.5, 130.5, 134.0, and 140.0 ppm), but regioirregular PTs show many resonances from 120 to 150 ppm.

PT derivatives can easily be synthesized by chemical oxidation methods [51]. In typical oxidation polymerization of PTs, 2,5-unsubstituted thiophenes, such as thiophene, 3-alkylthiophenes or 3-phenylthiophenes, etc., can be dissolved in CF, and, under an inert gas, the excessive oxidant ($FeCl_3$, $MoCl_5$, or $RuCl_3$) is added. The polymerization can take several hours. Generally, the $FeCl_3$ oxidation method has been widely used. The molecular weights of PTs prepared from this method range from 30 to 300 K, and the polydispersities range from 1.5 to 5.0. By this method, the regioregularities of poly(3-alkyl thiophene)s range from 70 to 80 %, whereas the regioregularity of poly(3-phenyl thiophene)s (P3PTs) can reach 90–95 %. The poor reproducibility is one of the major problems for oxidation polymerization reactions. As reported by Pomerantz et al. [52], the polymerization

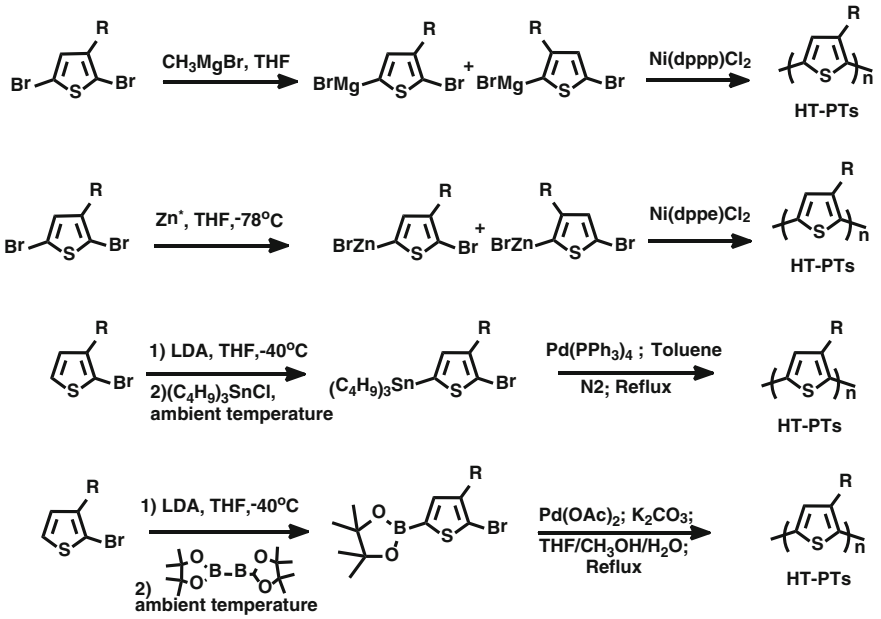

Fig. 5.9 Synthesis methods of regioregular poly(3-alkylthiophene)s by the McCullough and GRIM method, Rieke method, and the Stille and Suzuki coupling reactions

of 3-octylthiophene with $FeCl_3$ was repeated under identical reaction conditions five times, and the molecular weights of the five samples of poly(3-octylthiophene) ranged from 54 to 122 K with PDIs ranging from 1.6 to 2.7. Additionally, by using the identical preparation process, the polymer samples obtained from varied batches contain different levels of Fe impurities. Therefore, the oxidation method is seldom used to prepare PTs for applications in PSCs.

As shown in Fig. 5.9, regioregular poly(3-alkylthiophene)s can be prepared by various methods, such as the McCullough and GRIM method [53], the Rieke method [54], and the Stille [55] and Suzuki [56] coupling reactions. In 1992, McCullough et al. [53] reported the first synthesis method of head-to-tail coupled poly(3-alkylthiophene)s, and, from this method, close to 100 % HT-HT couplings. In this method, the monomer, 2-bromo-5-(bromomagnesio)-3-alkylthiophene, is obtained from 2-bromo-5-alkylthiophene at cryogenic temperature, and is then polymerized with catalytic amounts of $Ni(dppp)Cl_2$ (dppp is diphenylphosphinopropane). In this method, regioregular PTs were obtained in yields of 44–69 %. The Rieke method can also be used to synthesize regioregular poly(3-alkylthiophene) [54]. Regioselective control was realized on the basis of steric congestion at the reductive elimination step in the catalytic cycle. When the $Ni(dppe)Cl_2$ or $Ni(dppp)Cl_2$ was used as catalyst, the HT-couplings were more than 98.5 %. Other catalysts with less bulky, labile ligands such as PPh_3 combined with larger metal centers such as Pd lead to regiorandom poly(3-alkylthiophenes). The Stille [55] and Suzuki

[56] coupling methods are two convenient approaches to synthesize regioregular PTs, and these two methods exhibit great advantages in synthesis of multi-functional PTs because of the compatibilities of a large number of organic functional groups.

Regioregular poly(3-hexyl) thiophene (P3HT) is the most widely studied polymers in the field of PSC. The photovoltaic performance of P3HT/PCBM has been widely studied by numerous groups. It should be noted that the photovoltaic properties of P3HT/PCBM-based PSC devices are strongly dependent on the molecular weight and regioregularity of P3HT as well as the device fabrication methods [57–59]. Various strategies have therefore been developed to optimize the performance of P3HT-based polymer solar cells. In 2003, Sariciftci et al. [60] developed a postproduction treatment, namely, applying external voltage, which considerably improved the photovoltaic performance of solar cells based on the P3HT/PCBM system. Using this method, an enhancement of J_{sc} and an increase in external quantum efficiency (*EQE*) of 70 % are demonstrated. The breakthrough in the photovoltaic performance of P3HT/PCBM was realized by Li et al. [61] and Ma et al. [62] in 2005. Li et al. [61] developed a method of slow growth to optimize the morphology of P3HT/PCBM and an extremely high *PCE* of 4.4 % was realized, which was the highest value in the past decade. Alternatively, Ma et al. [62] applied post-production annealing at 150 °C, and P3HT/PCBM-based PSC devices with *PCE* approaching 5 % were achieved. In addition, these devices exhibited remarkable thermal stability. The improved performance was ascribed to the improved nanoscale morphologies, the increased crystallinities of P3HT, and the improved interfacial contact to the cathode, thereby enhancing the overall device efficiency. In 2010, He and Li et al. [63] introduced a novel fullerene acceptor, namely ICBA with a higher-lying LUMO level for the P3HT based polymers, which promoted the performance of P3HT to a new height by greatly increasing V_{oc}. After that, solvent additives and device engineering methods were utilized and increased the PCE of P3HT/ICBA to over 6.5 % [64, 65]. Clearly, the success of P3HT is largely associated with the active layer morphology [66, 67], such as using different casting solvents and film-forming speed, solvent and thermal annealing, etc.

Other P3HT-analogue polymers, for example poly(3-butylthiophene) (P3BT) and poly(3-pentylthiophene) (P3PT), were also explored in the device fabrications because of their similar crystalline and absorption characteristics. Nguyen et al. [68] investigated the effect of different alkyl lengths such as butyl, hexyl, octyl, decyl, and dodecyl on the photovoltaic properties of P3ATs-based PSC devices. Results revealed that longer alkyl chains (number of carbon atoms over 8) give poor efficiency and larger scale of phase separation. Jenekhe et al. [69] demonstrated that P3PT/PCBM-based BHJ PSC devices also give similar performances to those of P3HT/PCBM under the same conditions. Jenekhe and coworkers [70] also prepared P3BT nanowires and P3PT nanowires by solution-phase self-assembly, which were used to construct highly efficient P3AT/PCBM PSC devices. The fullerene/P3AT nanocomposite films showed an electrically bicontinuous nanoscale morphology and desirable *PCE* up to 3.3 %, which were identical with those of P3HT/PCBM-based

photovoltaic cells. Afterwards, Gadisa et al. [71] optimized the performance of P3PT/PCBM and a high *PCE* of 4.6 % was observed. Later, Li et al. [72] optimized the performance of P3PT with different fullerene acceptors. A *PCE* of 3.1 % and a *PCE* up to 5.4 % were achieved in P3PT/PCBM- and P3PT/ICBA-based PSC devices, respectively.

Two structurally related polymers of P3HT with high performance were developed by Hou and coworkers [73, 74]. Hou and Li et al. introduced conjugated side chains in PTs and developed a novel class of two-dimension (2D) conjugated polymers. A typical example among these 2D polymers is PTs with bi(thienyl-enevinylene) side chains. Three 2D conjugated PTs with bi(thienylenevinylene) side chains biTV-PTs (see PbTV in Fig. 5.7) were designed and synthesized by Hou and Li et al. in 2006 [73]. Compared with the properties of P3HT, the biTV-PTs show broad absorption bands (350–650 nm), much stronger absorbance, and lower HOMO levels. The *PCE* of the biTV-PT-based PSC devices reached ~3.2 %, which is ~40 % increased relative to that (~2.4 %) of the devices based on P3HT under the same conditions. This discovery expanded the scope of designing 2D conjugated polymers for efficient PSC devices.

Although photovoltaic performance as well as the photocurrent of P3HT can be improved via morphological optimizations, the low voltage (~0.6 V) is still the limiting factor of P3HT. In 2009, Hou et al. [74] also developed an easy and effective way to promote the V_{oc} of a poly(3-alkylthiophene) by reducing the number of alkyl chains of P3HT, and a novel P3HT-analogue polymer, P3HDTTT (see Fig. 5.7) with a V_{oc} up to 0.82 V was obtained. In 2011, Li et al. [75] also introduced carboxylate substituent in polythiophene derivatives to tune downward the HOMO of polythiophene. A novel polythiophene derivative of PT-C3 (see Fig. 5.7) was also synthesized and characterized. The PSCs based on PT-C3/$PC_{71}BM$ exhibited relatively high V_{oc} of ~0.8 V. The *PCE* of the PSCs based on PT-C3 reached 3.87 % with V_{oc} = 0.78 V, J_{sc} of 9.68 mA cm^{-2}, and *FF* of 51.2 % under the illumination of AM1.5G, 100 mW/cm^2. These studies indicated that, in respect of further enhancing the J_{sc}, P3HDTTT would be a potential polymer to replace P3HT as blue absorber in tandem PSC devices.

5.2.2 Donor–Acceptor Copolymers

5.2.2.1 Benzothiadiazole (BT)-Based Polymers

D–A copolymers based on BT and its derivatives (see the molecular structures and photovoltaic parameters in Fig. 5.10 and Table 5.3) were explored because the HOMO and LUMO energy levels as well as band gaps can been effectively tuned by choosing donor (D) and acceptor (A) building blocks with appropriate electron-donating or -accepting natures. In 2003, the fluorene (FL) and benzothiadiazole (DTBT) copolymer, PFDTBT, was synthesized by Andersson and coworkers [76], which was generally considered as one of the first reports of donor–acceptor (D–A)

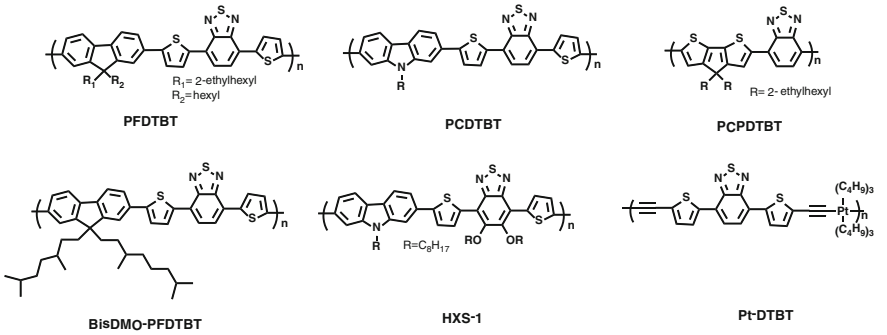

Fig. 5.10 Molecular structures of D–A copolymers based on benzothiadiazole

Table 5.3 Photovoltaic results of D–A copolymers based on benzothiadiazole

Materials	V_{oc} (V)	J_{sc} (mA/cm^2)	FF (%)	PCE (%)	μ_h [cm^2/(Vs)]	Ref.
BisDMO-PCDTBT	0.97	9.1	51	4.5	3×10^{-5}	[77]
PCPDTBT	0.62	16.2	55	5.5	–	[79]
PCDTBT	0.89	6.9	56	3.6	3×10^{-3}	[80]
HXS-1	0.81	9.6	69	5.4	–	[83]
Pt-DTBT	0.80	15.1	40	4.8	–	[84]

conjugated polymers. In this work, PFDTBT exhibited poor solubility but reached a moderate *PCE* of 2.2 %. Although the *PCE* was not high, the D–A copolymer exhibited potentials such as LBGs and tunable energy levels. Following the pioneer work of Andersson et al., numerous novel D–A copolymers based on different donor units and acceptor units were synthesized and utilized in PSC devices. It should be noted that D–A copolymers have been the most successful class of polymer photovoltaic materials for PSCs in recent years.

Considering the V_{oc} of this polymer is as high as 1 V, the performance of PFBTBT still has a large promotion space. In 2008, Hou et al. [77] altered the alkyl chains in the classical PFDTBT backbone. Two novel polymers, bisEH-PFDTBT and bisDMO-PFDTBT, employing the same polymer backbone as PFDTBT but different side chains, were studied to investigate the side-chain effects. After carefully optimizing the side chains, the *PCE* of bisDMO-PFDTBT was increased to 4.5 %. Notably, the saturated alkyl chains have little influence on the molecular energy levels of PFDTBT. From quantum-chemical calculations, both the ethyl groups are in the proximity of the conjugated backbone, and thus decreased the probability of π–π stacking in bisEH-PFDTBT originating from the steric effect. In contrast, there are two small methyl groups located on the third and seventh carbons of the bisDMO-PFDTBT which not only decrease the steric effect but also increase the solubility and hole mobility.

The cyclopentadithiophene and DTBT copolymer, PCPDTBT, is also a well-known LBG D–A copolymer, which was developed by Brabec et al. [78] in 2006. PCPDTBT is the first LBG polymer with high efficient photovoltaic activity in the IR spectral region. In 2008, Bazan et al. [79] introduced solvent additive 1,8-octanedithiol (OT) to optimize the nanomorphology of this polymer, and a twofold enhancement was observed. A high *PCE* of 5.5 % was recorded and regarded as a milestone of novel photovoltaic polymers. It should be noted that PCPDTBT is an amorphous polymer. The approach provided a feasible tool for modulating the heterojunction morphology in donor/acceptor systems where thermal annealing is not effective.

Another representative D–A copolymer is PCDTBT, which was copolymerized by carbazole (CZ) and DTBT by the Leclerc group [80]. PCDTBT had a low-lying HOMO level of −5.45 eV and a moderate band gap of 1.88 eV. A preliminary *PCE* of 3.6 % was measured at a donor/acceptor weight ratio of 1:4. Various methods were proposed to optimize the photovoltaic properties of PCDTBT. Notably, PCDTBT is among the most efficient, stable, and low-cost photovoltaic materials for PSC devices with a high V_{oc} (0.85–0.90 V), high *PCE* (6–7 %), and long lifetime (∼7 years), which is now considered to be one of the new benchmarks for the development of highly efficient BHJ solar cells [81, 82]. Afterwards, Bo et al. [83] optimized the side chains of DTBT; a novel polymer, HXS-1 with planar configuration, achieved a high *PCE* over 5 % and excellent *FF* approaching 70 %.

A platinum metallopolyyne (herein called Pt-DTBT) with a LBG of 1.85 eV was also reported by Wong et al. [84]. The PSCs based on the metallated polymer exhibited an average *PCE* of 4.1 % without annealing. It is noteworthy that the devices based on the Pt-DTBT/PCBM system exhibited a very high J_{sc} of ∼15 mA/cm^2 and relatively high V_{oc} of ∼0.80 V. This is the first time that a metallated polymer was applied in PSC devices to get such a high *PCE*.

5.2.2.2 Silole-Containing Polymers

Fused coplanar thiophene-based heterocycles, such as dithieno[3,2-*b*:2′,3′-*d*]silole (DTS) and IDT, have been actively utilized as donor units to construct novel D–A copolymers. To optimize the photovoltaic performance of D–A copolymers as discussed above, such as PFDTBT and PCPDTBT, silole-containing building blocks, such as silafluorene (SiF) and dithienosilole (DTS), have been widely utilized in efficient D–A polymers. In the following we overview the representative polymers in the third generation. The majority of these polymers exhibited high *PCE* ranging from 5 to 7 %.

Cao and coworkers [85] successfully introduced the silicon atom into FL units and copolymerized the novel SiF unit and 4,7-di(2′-thienyl)-2,1,3-benzothiadiazole (DTBT). High-performance polymer solar cells composed of an alternating copolymer PSiF-DBT as the electron donor and $PC_{71}BM$ as the electron acceptor were investigated. A high *PCE* up to 5.4 % with a high V_{oc} of 0.90 V, a J_{sc} of 9.5 mA cm^{-2}, and a *FF* of 50.7 % was achieved under the illumination of AM

1.5*G* 80 mW/cm^2. Moreover, PSiF-DBT also showed a high hole mobility of ~1 × 10^{-3} cm^2 V^{-1} s^{-1}. Bo and coworkers [86] optimized the side chains in DTBT of the PSiFDBT, and obtained an improved *PCE* of up to 6.05 %. Driven by the high performance of PCPDTBT and PSiFDBT, Hou et al. [87] designed and synthesized a LBG DTS-containing polymer, PSBTBT. The preliminary *PCE* obtained with thermal annealing (140 °C, 5 min) was 5.1 % and then was increased to ~5.6 %. Chen et al. [88] further revealed the origin of the high performance of PSBTBT relative to PCPDTBT. Striking morphological changes were observed in polymer: fullerene bulk heterojunctions upon the substitution of the bridging atom. GIXRD investigations indicated increased π–π stacking in silole-based polymers compared to the carbon-bridged analogue [89, 90]. More importantly, the response range of the PSBTBT covered the whole visible range from 380 to 800 nm, which indicated that PSBTBT is an efficient red-absorbing polymer for tandem PSCs. Benefitting from the broad absorption (300–800 nm), *PCE* values up to 7 % were achieved in tandem PSC devices by the Yang group and others.

Afterwards, various units were copolymerized with these silole-containing building blocks and a class of low-band gap polymers was developed. Their molecular structure and photovoltaic parameters are depicted in Fig. 5.11 and Table 5.4. In particular, DTS-based copolymers show a broad absorption, relatively lower HOMO energy level, and higher hole mobility, which are attractive for

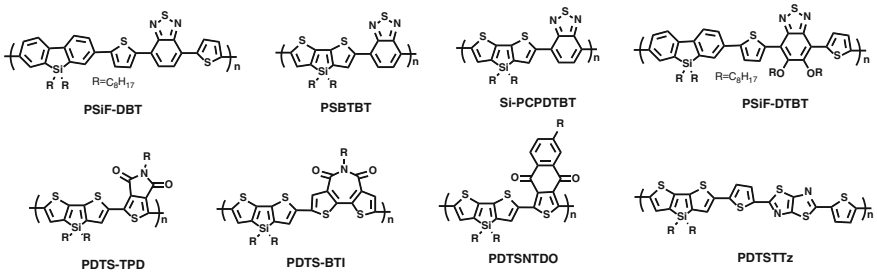

Fig. 5.11 Molecular structures of silole-containing polymers

Table 5.4 Photovoltaic results of silole-containing polymers

Materials	V_{oc} (V)	J_{sc} (mA/cm^2)	FF (%)	PCE (%)	μ_h [cm^2/(Vs)]	Ref.
PSiF-DBT	0.90	9.5	50.7	5.4	1 × 10^{-3}	[85]
PSiF-DTBT	0.91	11.5	58	6.05	3.2 × 10^{-3}	[86]
PSBTBT	0.68	12.7	55	5.1	3 × 10^{-3}	[87]
Si-PCPDTBT	0.58	14.92	61	5.24	1 × 10^{-3}	[89]
PDTSTTz	0.77	11.9	61	5.59	3.56 × 10^{-3}	[91]
PDTSNTDO	0.88	9.24	64	5.21	–	[92]
PDTS-BTI	0.80	12.81	62.3	6.41	–	[93]
PDTSTPD	0.88	12.2	68	7.3	1 × 10^{-4}	[94]

researchers. Considering that the thiazolothiazole (TTz) unit has a rigid and coplanar configuration and thereby ensures a highly extended π-electron system and strong π–π stacking, Zhang et al. [91] copolymerized DTS with the TTz acceptor unit. The *PCE* of the PSC based on PDTSTTz/$PC_{71}BM$ (1:1, wt/wt) reached 5.59 % with V_{oc} = 0.77 V, J_{sc} = 11.9 mA/cm^2, and *FF* = 61 % under optimized conditions (thermal annealing at 100 °C for 15 min). Cui et al. [92] designed a strong electron-withdrawing unit, naphtho[2,3-*c*]thiophene-4,9-dione, which was copolymerized with DTS to construct a D–A copolymer, PDTSNTDO, with a narrow band gap and lower lying HOMO level. The *PCE* of the PDTSNTDO-based device reached 5.21 %, with a high V_{oc} of 0.88 V.

Marks et al. [93] synthesized a new series of bithiopheneimide (BTI)-based donor–acceptor copolymers for efficient PSCs. Among these, PSC featuring BTI and DTS copolymer as donor and $PC_{71}BM$ as acceptor exhibited promising device performance with *PCE* up to 6.41 % and high V_{oc} over 0.80 V. The BTI analogue, TPD-based device exhibited 0.08 V higher V_{oc} with an enhanced *PCE* of 6.83 %, which is mainly attributed to the lower-lying HOMO induced by the higher imide group density in the backbone. Lu and Tao et al. [94] recently synthesized a new D–A copolymer PDTSTPD of DTS and thienopyrrole-4,6-dione (TPD) obtaining both a LBG (1.73 eV) and a deep HOMO level of −5.57 eV. When blended with $PC_{71}BM$, PDTSTPD exhibited an excellent *PCE* of 7.3 % on the photovoltaic devices with an active area of ∼1 cm^2. These results demonstrate the great potential of DTS-based polymers for high-performance solar cells, and provide valuable insights into structure-property relationship of atom substitution.

5.2.2.3 Diketopyrrolopyrrole (DPP)-Based Polymers

As one of the high-performance pigments, the DPP unit was developed in the past few decades for constructing LBG (1.5 eV) conjugated polymers produced by its strong electron-withdrawing properties. Another attractive property of DPP is its excellent charge carrier mobility for both holes and electrons. Most of the photovoltaic performance of DPP-based polymers is likely to depend on its solvent-induced morphology [32].

Janssen et al. [95] introduced DPP unit in D–A copolymers in 2008. Dozens of newly designed DPP-based LBG polymers have been frequently reported since 2009. The molecular structure and photovoltaic parameters of these DPP based polymers are depicted in Fig. 5.12 and Table 5.5. Hou et al. [96] copolymerized DPP with various electron-donating monomers and obtained a series of new LBG polymers based on the DPP unit. Among these DPP-based polymers, benzodithiophene and DPP copolymer, PBDT-DPP showed a small band gap of 1.34 eV and a moderate *PCE* of 4.45 % was achieved.

When copolymerizing DPP with thiophene and the like, ultra-LBG (E_g ∼1.3 eV) polymers such as PDPP3T [34] and PDPP3MT [97] can be obtained. The first highly performing DPP-containing polymer, PDPP3T, was synthesized [34] and applied in organic photovoltaic and field-effect transistor devices by Janssen et al. in 2009. After

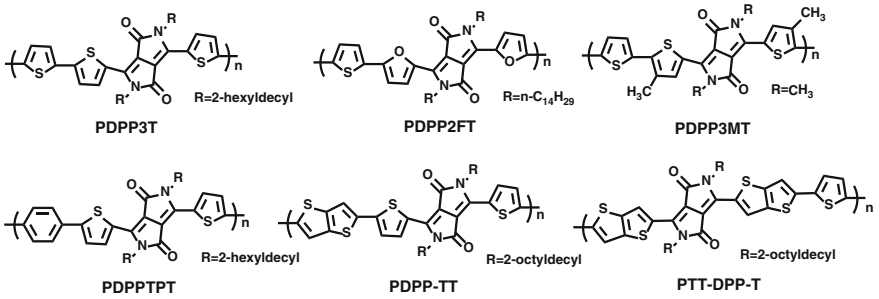

Fig. 5.12 Molecular structures of representative DPP-based efficient polymers

Table 5.5 Photovoltaic performances of the representative D–A copolymers based on DPP units

Copolymers	V_{oc} (V)	J_{sc} (mA/cm^2)	FF (%)	PCE (%)	μ_h [cm^2/(Vs)]	Ref.
PDPP3T	0.66	15.41	65.92	6.71	3.9×10^{-3}	[35]
PDPP3MT	0.60	17.8	66	6.8	–	[97]
PTT-DPP-T	0.58	15	61	5.4	–	[98]
PDPP2T-TT	0.66	14.8	70	6.9	–	[100]
PDPPTPT	0.80	10.8	65	5.5	–	[101]
PDPP2FT	0.65	14.8	64	6.5	7×10^{-4}	[102]

optimizing processing solvent and molecular weight, the moderate *PCE* of 4.7 % was increased to 6.7 % by Ye et al. [35] and 7.0 % by Janssen et al. [97]. To tune the coplanarity of PDPP3T, Janssen et al. [97] introduced methyl into the thiophene group of DPP unit, and a higher performance ultra-LBG polymer PDPP3MT was achieved with *PCE* of 6.8 % in the classic device configuration. Bronstein et al. [98, 99] reported the synthesis and polymerization of a novel thieno[3,2-*b*]thiophene-DPP-based building block in recent years. Copolymerization with thiophene afforded the resulting polymer, PTT-DPP-T, with a high hole mobility of 1.95 cm^2 V^{-1} s^{-1}. PSC devices comprised of PTT-DPP-T and $PC_{71}BM$ also exhibited an excellent *PCE* of 5.4 % and high J_{sc} up to 15 mA/cm^2 [98]. Later, Li et al. [100] designed a high-molecular-weight conjugated polymer based on an alternating electron-rich TT unit and an electron-deficient DPP unit, which also provided efficient polymer solar cells with *PCE* up to 6.9 %. The optimal morphology of the new polymer/PCBM blend reduced bimolecular recombination and thereby allowed a high *FF* up to 70 % and high *PCE*s over 6 % with film thickness up to 300 nm to be achieved. Because of the lower π-electron density of the benzene unit compared with thiophene, the DPP and benzene copolymer, PDPPTPT [101], showed a relatively higher band gap of 1.53 eV and lower HOMO level (−5.35 eV) together with a broad photo-response range up to 800 nm. When blended with $PC_{71}BM$, higher *PCE* of 5.5 % with $J_{sc} = 10.8$ mA/cm^2, $V_{oc} = 0.80$ V, and $FF = 65$ % was achieved. Clearly, PDPPTPT is a suitable photovoltaic polymer for multi-junction devices because of the balance between the broad absorption range and high voltage.

Frechet et al. [102, 103] developed a series of furan-containing DPP-based polymers, such as PDPP2FT and PDPP3F, with substantial power conversion efficiencies. Inserting furan into the backbone of the conjugated polymers enables the utility of relatively small solubilizing alkyl chains because of the significant contribution of the furan to overall polymer solubility in common organic solvents. PSC devices fabricated from PDPP2FT and $PC_{71}BM$ as active layers showed a high *PCE* reaching 6.5 % [102]. The design and synthesis of the successful examples of furan-containing LBG polymers paved the way to developing environmental photovoltaic polymers. Interestingly, it is also noted that furan-containing LBG polymers with high side-chain tunability also provide insights into molecular order in efficient PSCs. In recent years, the *PCE* of DPP based polymers was also increased to exceed 7 % by the Janssen group [104] and the Yang group [9–11] because of the molecular weight and side chain optimization. These highly efficient polymers are introduced in the fourth generation. Moreover, these red absorber materials exhibited potential applications in tandem and triple junction PSCs.

5.2.2.4 Indacenodithiophene (IDT)-Based Polymers

Ladder type units such as IDT, also known as thiophene-phenylene-thiophene (TPT), constitute a class of efficient D–A copolymers, which have been emerging as efficient building blocks since 2008 [105, 106]. Typically, the IDT unit is extremely versatile with a coplanar aromatic ring structure, and the electron density can be manipulated by the choice of the bridging group between the rings. The coplanarity of the IDT unit could enhance interchain interaction of the polymers and is expected to afford higher hole mobility. Ting et al. pioneered the IDT-based random and alternating copolymers for photovoltaic applications [107, 108]. In 2008, two LBG IDT-based polymers with high hole mobility (3.4×10^{-3} cm^2 V^{-1} s^{-1}) were designed and synthesized for application in PSCs by Ting and coworkers [106]. High-performance *PCE* of 4.4 % was obtained, which was superior to that of the analogous P3HT based PSC device under the same device fabrication condition. In 2010, Ting and collaborators [108] also synthesized an alternating copolymer (a-PTPTBT) based on IDT and BT and the highest *PCE* reached 6.4 % of the corresponding PSC under the optimal condition of solvent vapor annealing. The molecular structure and photovoltaic parameters of the representative IDT based polymers are depicted in Fig. 5.13 and Table 5.6.

Jen et al. [109] first applied aryl side chain substituted IDT in quinoxaline-based conjugated polymers and combined IDT and two quinoxaline derivatives to form novel polymers (PIDT-diphQ and PIDT-phanQ; Fig. 5.13). Because of the enhanced planarity of phenanthrenequinoxaline (phanQ), PIDTphanQ/$PC_{71}BM$-based PSC device exhibited an improved *PCE* of 6.24 % compared to the *PCE* of 5.69 % in PIDT-diphQ/$PC_{71}BM$-based device. Jen et al. also developed several high-performance IDT-based D–A copolymers such as PIDT-DFBT [110, 111]. Huang, Cao and coworkers [112] synthesized three low band-gap conjugated polymers via Stille copolymerization of IDT and naphtho[1,2-*c*:5,6-*c*]

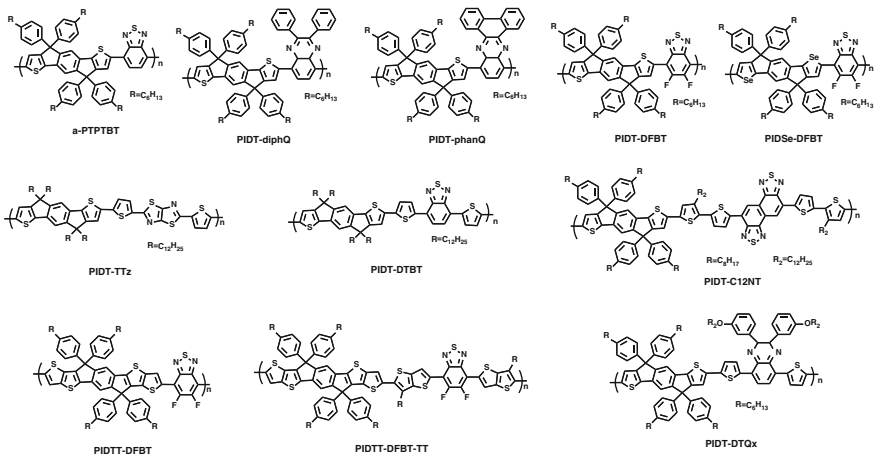

Fig. 5.13 Molecular structures of the representative IDT-based efficient polymers

Table 5.6 Photovoltaic results of the representative IDT-based polymers

Materials	V_{oc} (V)	J_{sc} (mA/cm^2)	FF (%)	PCE (%)	μ_h [cm^2/(Vs)]	Ref.
a-PTPTBT	0.85	11.2	67.2	6.41	2.4×10^{-5}	[108]
PIDT-diphQ	0.87	10.9	60	5.69	1.14×10^{-3}	[109]
PIDT-phanQ	0.87	11.2	64	6.2	2.06×10^{-3}	[109]
PIDT-DFBT	0.97	11.2	55	5.97	4×10^{-5}	[111]
PIDT-C12NT	0.90	10.21	55	5.05	2.42×10^{-4}	[112]
PIDT-TTz	0.89	13.3	48.9	5.79	4.99×10^{-3}	[113]
PIDT-DTBT	0.82	12.27	56.7	6.17	2.24×10^{-3}	[113]
PIDSe-DFBT	0.89	13.7	56.3	6.8	0.15	[114]
PIDTT-DFBT	0.95	12.21	61	7.03	3×10^{-4}	[111]
PIDTT-DFBT-TT	0.96	11.9	63	7.2	4×10^{-2}	[111]
PIDT-DTQx	0.87	12.34	70.23	7.51	1.18×10^{-4}	[115]

bis(1,2,5-thiadiazole) (NT) based monomers. The energy levels, absorption spectra, and band gaps of the target polymers were well tuned by utilizing different thiophene derivatives as spacer between IDT and NT units, and polymer PIDT-C12NT which employed bithiophene attached with dodecyl side chain as spacer exhibited superior properties compared with the other two copolymers. All polymers exhibited deep HOMO levels and subsequently led to high open circuit voltages of the fabricated PSC devices. The best performance (5.05 %) was achieved with PIDT-C12NT as donor polymer, which can be ascribed to its higher hole mobility, the optimal interpenetrating network, as well as enhanced absorption coefficient with respect to the other two polymers. The photovoltaic results demonstrated that the combination of IDT and NT with appropriate spacers might be a promising approach for the application of solar cells.

Considering potentials of the alkyl-substituted IDT, such as good planarity, good solubility, and high hole mobility, Zhang et al. [113] copolymerized alkyl-substituted IDT with different acceptor units including bithiazole (BTz), thiazolothiazole (TTz), tetrazine (TZ), and benzothiadiazole (DTBT). Among these copolymers, PIDTTTz has the highest hole mobility of 4.99×10^{-3} cm^2 V^{-1} s^{-1} and the *PCE* of the PSC based on PDTSTTz/$PC_{71}BM$ reached 5.79 % with a V_{oc} of 0.89 V, a J_{sc} of 13.3 mA/cm^2, and a *FF* of 48.9 %, under the donor/acceptor component ratio of 1:2 (wt/wt). In comparison with PIDT-TTz, PIDT-DTBT has a medium band gap of 1.68 eV and a similar hole mobility of 2.24×10^{-3} cm^2 v^{-1} s^{-1}. The PSC based on PIDT-DTBT/$PC_{71}BM$ reached an even higher *PCE* of 6.17 %. These results indicated that the D–A copolymers based on the alkyl-substituted IDT unit are promising photovoltaic polymer materials because of the excellent hole mobility and solubility as well as deeper HOMO levels. The selenophene and other analogues of IDT were developed in recent years. For instance, Jen et al. [114] improved the molecular weight of IDSe-based polymers and a high *PCE* up to 6.8 % was recorded for a PIDSe-DFBT-based PSC device, which exhibited over 10 % enhancement compared to that of a PIDT-DFBT-based PSC device. This work demonstrated that selenium substitution on the IDT is an effective method to reduce the band gap and improve the photovoltaic performance of IDT-based polymers with higher molecular weight.

Recently, several IDT-based polymers realized high *PCE*s over 7 % and exhibited unique charge transport properties. For instance, Jen et al. [111] incorporated TT moiety in IDT unit and designed an IDTT unit. Utilizing IDTT unit in DFBT and TT bridged DFBT-based polymers, corresponding copolymers PIDTT-DFBT and PIDTT-DFBT-TT with *PCE* up to 7 % as well as V_{oc} over 0.95 V were observed. Hou et al. [115] incorporated IDT with DTQx and produced a highly efficient polymer PIDT-DTQx with a *PCE* up to 7.5 %, which was the highest value in IDT-based copolymers. Interestingly, PIDT-DTQx exhibited the best performance under the donor/acceptor weigh ratio of 1:4.

5.2.2.5 Benzodithiophene (BDT)-Based Polymers

Although various efficient photovoltaic polymers have been developed, the polymers discussed above (*PCE* < 7 %) still could not meet the need of commercial requirements. In this part, we overview the representative highly efficient photovoltaic polymers. In particular, the rapid progress of benzo[1,2-*b*:4,5-*b*′]dithiophene (BDT) and two dimensional BDT-based polymers are introduced. These polymers with *PCE* over 7 % draw lots of attention from both the industrial and the academic communities.

Benzodithiophene (BDT) has a large planar conjugated structure and easily forms π–π stacking, and thereby improves the hole mobility [116]. In 2008, Hou et al. [117] first introduced the BDT unit in the synthesis and application of photovoltaic polymers. In the work, alkoxy-substituted BDT was copolymerized with seven different units. The band gap and absorption spectrum of the BDT-based

polymers could be effectively tuned within a wide range. In 2009, Yu and coworkers copolymerized BDT with thieno[3,4-*b*]thiophene (TT) and designed a series of BDT-TT copolymers, namely the PTB series [118–120]. Among these PTB series polymers, PTB7 [120] is the best-performing photovoltaic polymer because of the optimal side chain and functional substituents. Hou et al. also designed a series of BDT and TT copolymers, such as PBDTTT-C [121], PBDTTT-CF [122], and PBDTTT-S [123]. It should be mentioned that PBDTTT-CF and PTB7 are the first two polymers with *PCE* exceeding 7 %, which significantly pushes the PSC research to a new height. Following this pioneering work, *PCE*s of more than 7 % were frequently reported in various groups, as depicted in Fig. 5.14. The photovoltaic results of the corresponding polymers are listed in Table 5.7.

Besides TT, numerous building blocks including DPP, thieno[3,4-*c*]pyrrole-4,6-dione (TPD), benzothiadiazole (BT), and benzoxadiazole (BO) have been

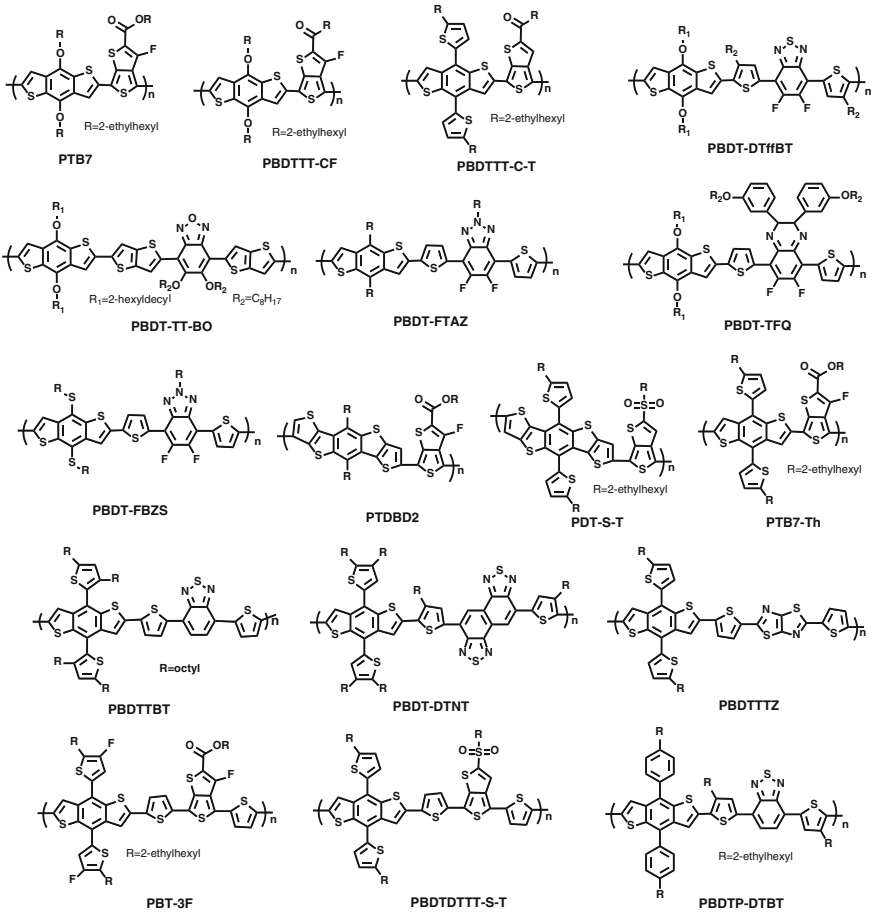

Fig. 5.14 Molecular structures of BDT-based highly efficient polymers

Table 5.7 Photovoltaic performance of the representative D–A copolymers based on BDT and BDT analogues

Materials	V_{oc} (V)	J_{sc} (mA/cm^2)	FF (%)	PCE (%)	μ_h [cm^2/(Vs)]	Ref.
PBDTTT-CF	0.76	15.2	66.9	7.73	7×10^{-4}	[122]
PTB7	0.74	14.5	68.97	7.4	5.8×10^{-4}	[120]
PBnDTDTffBT	0.91	12.91	61.2	7.2	8.3×10^{-3}	[124]
PBDT-FTAZ	0.79	12.45	72.2	7.1	1.03×10^{-3}	[125]
PBDTDTBTff-3	0.78	15.38	69.2	8.30	–	[126]
PBDT-TT-BO	0.76	13.87	66.6	7.05	0.023	[128]
PBDT-TFQ	0.76	18.2	58.1	8.0	–	[129]
PBDTFBZS	0.88	12.36	71.2	7.74	4.3×10^{-3}	[127]
PBDTTT-C-T	0.74	17.48	58.7	7.59	0.27	[131]
PBDTDTTT-S-T	0.70	17.07	66.3	7.81	2.76×10^{-3}	[132]
PBDTT-SeDPP	0.69	16.8	62	7.2	6.9×10^{-4}	[10]
PBDTP-DTBT	0.88	12.94	70.9	8.07	8.89×10^{-2}	[139]
PBDTTBT	0.92	10.7	57.5	5.66	–	[130]
PBDTTTZ	0.85	10.4	59.0	5.22	1.67×10^{-5}	[138]
PBDTDTNT	0.80	11.71	61.0	6.00	3×10^{-5}	[137]
PBT-3F	0.78	15.2	72.4	8.6	–	[140]
PDT-S-T	0.73	16.63	64.13	7.79	–	[143]
PTDBD2	0.89	13.0	65.3	7.6	–	[144]

successfully combined with the BDT unit to constitute highly efficient photovoltaic polymers.

You and collaborators [124] reported the first successful application of fluorinated benzothiadiazole in BDT-based polymers. The resulting polymer PBDTDTffBT exhibited down-shifted HOMO and LUMO energy levels and a similar band gap relative to its non-fluorinated analogue. As a result, the PSC device employing PBDTDTffBT achieved a greatly improved *PCE* of 7.2 %. Similarly, fluorine was incorporated into 2-alkyl-benzotriazoles (TAZ) by You et al. [125] and a novel polymer PBnDT–FTAZ was designed. Interestingly, although the band gap of fluorinated polymer PBnDT–FTAZ was ~2.0 eV, the copolymer exhibited a *PCE* above 7 % when mixed with $PC_{61}BM$, and a *PCE* above 6 % was still attained even for thickness up to 1 μm. The superior performance originated from their high hole mobility and low HOMO and LUMO levels. Very recently, Wang et al. [126] successfully optimized the similar fluorinated benzothiadiazole-based conjugated copolymers, PBDTDTBTff, with different side chains. A *PCE* up to 8.30 % was achieved in PBDTDTBTff-3-based PSC devices with ~100 nm thickness active layers without any processing additives or post-treatments, which was the highest value for the conventional single-junction polymer solar cells via simple fabrication architecture. In addition, it is noteworthy that PBDTDTBTff-3 could afford high *PCE*s of 7.27 % at ~200 nm thickness active layers and 6.56 %, even for thicknesses up to ~300 nm. Therefore, the results demonstrated that BDT

and fluorinated benzothiadiazole polymers should be promising candidates for developing high-performance large-scale roll-to-roll fabrication of PSCs.

Peng et al. [127] further applied dialkylthiol-substituted BDT in the synthesis of conjugated copolymers based on monofluorinated benzotriazole (TAZ) acceptor block, and a high-performance PBDTFBZS was developed. As expected, wide band-gaps and deep HOMO and LUMO energy levels were observed in the resulting copolymers. A *PCE* up to 7.74 % was achieved from the regular single device based on PBDTFBZS with a V_{oc} = 0.88 V, a J_{sc} = 12.36 mA/cm^2 as well as a high *FF* of 71.2 %. The enhanced V_{oc} can be ascribed to a low-lying HOMO energy level by the introduction of dialkylthiol and fluorine substituents on the PBDT-DTBT polymer backbone. The improvements in J_{sc} *FF* are probably because of high hole mobility, suppressed charge recombination, and optimal blend morphology. Because of the excellent performance of polymers, tandem PSC devices featuring PBDTFBZS as blue absorber material and DPP-based polymer as red absorber material exhibited high *PCE* up to 9.40 %. Compared to BT-based polymers, benzoxadiazole (BO)-based polymers exhibited a rather disappointed performance. Very recently, to overcome the relatively poor performance and low solubility of BO-based polymers, Li and coworkers [128] designed a TT-bridged polymer, namely, PBDT-TT-BO, which was copolymerized by BDT unit and TT-bridged BO acceptor unit. The *PCE* of the PSC device featuring PBDT-TT-BO as donor polymer reached 7.05 %, which was the champion result in BO containing conjugated polymers and comparable to that of its BT counterparts. A medium-band gap fluorinated quinoxaline-based conjugated polymer of PBDT-TFQ was designed and synthesized by Chou and coworkers [129]. With an optimized blend ratio of PBDT-TFQ:$PC_{71}BM$ (1:1, wt/wt), a high *PCE* of 8.0 % was obtained, with a V_{oc} of 0.76 V, a J_{sc} of 18.2 mA/cm^2, and a *FF* of 58.1 %. The resulting copolymer achieved an extremely high J_{sc}, which was probably caused by the higher hole mobility of PBDT-TFQ together with the better morphology for efficient exciton dissociation and charge transport.

In recent years, a large class of donor–acceptor copolymers based on the two-dimensional conjugated BDT units (collectively called 2D-BDT units) was developed by Hou and coworkers [130–136]. In 2010, Huo et al. [130] copolymerized thiophene bridged 2,1,3-benzothiadiazole (BT) with an alkylthienyl-substituted BDT unit, and the first 2D-BDT-based polymer, PBDTTBT with V_{oc} up to 0.92 V and *PCE* over 5.6 % was achieved. By introducing the 2D-BDT units such as alkylthienyl substituted BDT, the *PCEs* of several novel polymers, including PBDTTT-C-T, PBDTTDTT-S-T, PBDTP-DTBT, and PBT-3F, have been increased to 8–9 % in Hou's group. A typical example is PBDTTT-C-T. Huo et al. [131] replaced the alkyl chain with an alkylthienyl side chain in the BDT unit of PBDTTT-C, which resulted in a high-performance polymer PBDTTT-C-T. Notably, PBDTTT-C-T has been widely utilized in versatile photovoltaic devices such as inverted devices because of its excellent properties. The 2D-BDT design rules were also successfully applied to more than three pairs of BDT-based systems [132–136]. Two donor–acceptor conjugated polymers, PBDT-DTBT and PBDT-DTNT, based on 2,1,3-benzothiadiazole (BT) and naphtho[1,2-*c*:5,6-*c*]bis [1, 2, 5]

thiadiazole (NT), have been designed, synthesized, and characterized by Huang and collaborators [137]. Compared with BT, NT contains two fused 1,2,5-thiadiazole rings which narrow the band gap, enhance the interchain packing, and improve the charge mobility of the resulting polymer. Consequently, the NT-based polymer PBDT-DTNT exhibited considerably better photovoltaic performance with a *PCE* of 6.00 %, which is significantly higher than that of the BT-based polymer PBDT-DTBT under identical conditions. Huo et al. [138] also synthesized a wide band gap BDTT-based polymer, PBDTTTZ, and achieved a desirable *PCE* of 5.21 %, which is one of the highest among wide band gap (>2 eV) polymers. Considering that the absorption edge of the PBDTTTZ is 620 nm, which is ~20 nm shorter than that of P3HT, PBDTTTZ should be an excellent blue absorber for tandem devices relative to P3HT. Clearly, the impressive performance of BDT-based polymers has shown its obvious potential for achieving high performance in PSCs. The photovoltaic results demonstrated that photovoltaic polymers based on 2D-BDT units exhibited improved hole mobilities, and significantly improved photovoltaic performance relative to those of their corresponding alkoxy-substituted BDT-based photovoltaic polymers. Therefore, replacing BDT with 2D-BDT units should be a method to enhance the efficiency with wide applicability.

Similarly, Chen et al. [12] recently introduced the alkylthienyl side chain in the BDT unit of PTB7-Th, which produced a significantly improved *PCE* (~9.35 %) relative to PTB7 under the same conditions. Yang et al. [9–11] incorporated the 2D-BDT unit in the DPP based polymers, and high-performance low band-gap polymers such as PBDTT-DPP [9] and, PBDTT-SeDPP [10] were designed and synthesized. These PBDTT-DPP materials played vital roles in versatile highly efficient semi-transparent and tandem PSC devices. It is worth mentioning that the tandem devices incorporating PBDTT-DPP as LBG absorbing polymers have increased the *PCE* to a new height (PCE > 9 %) and have drawn worldwide attention.

Recently, alkylphenyl substituted BDT (BDT-P) has attracted much attention as a weak electron-donating unit with a large π-conjugated area and good planarity. Yang and coworkers [11] reported a series of copolymers based on BDT-P for photovoltaic application. Results revealed that BDT-P-based polymers exhibit similar photovoltaic performance and relatively higher V_{oc} in comparison with polymers based on alkylthienyl substituted BDT. Afterwards, Zhang et al. [139] designed and synthesized a novel copolymer PBDTP-DTBT based on benzothiadiazole and BDT-P. The best-performing PSC device based on PBDTP-DTBT/$PC_{71}BM$ (1:1.5, wt/wt) reached a *PCE* up to 8.07 % with a V_{oc} = 0.88 V, a J_{sc} = 12.94 mA/cm^2, and a *FF* = 70.9 % under the irradiation of AM 1.5G, 100 mW/cm^2. Interestingly, with only 0.5 vol.% DIO, the PBDTP-DTBT-based D/A blends exhibited the best performance because of the well-tuned morphology. Although the DIO volume was higher than 1 %, the *PCE* was greatly reduced to a moderate value (<7 %). To ameliorate the relatively low voltage in alkylthienyl-substituted BDT and thiophene-bridged TT-based copolymers, Zhang et al. [140] further demonstrated the synergistic effect of introducing fluorine (F) atoms of lowering the molecular energy levels, HOMO and LUMO levels of copolymers of alkylthienyl substituted BDT and thiophene-bridged TT. When three F atoms were

introduced in both the donor and acceptor units, the PSC device based on the trifluorinated polymer (PBT-3F) showed an extremely high *PCE* of 8.6 % and a significantly improved V_{oc} of 0.78 V, which was the efficiency record for PSCs utilizing the classic device configuration. This work demonstrated that introducing F onto the appropriate positions of the donor units in D–A polymers, especially BDT-based polymers, is a promising method to modulate effectively the molecular energy levels for better applications in PSCs.

Driven by the great success of BDT, various BDT analogues were designed and synthesized for producing high-performance D–A copolymers [141–144]. For instance, Hou et al. [142] designed a novel BDT analogue, namely DTBDT, and synthesized a series of DTBDT-based copolymers. Among these polymers, PDT-S-T [143] exhibited the best performance with *PCE* up to 7.79 % because of favorable and ordered molecular packing originating from the linear conformation of the backbone. Yu et al. [144] copolymerized DTBDT and TT, and a highly efficient polymer, PTDBD2, with *PCE* over 7.5 % was obtained. The V_{oc} of the PTDBD2-based PSC device is as high as 0.89 V, which is remarkably higher than that (0.74 V) of the PTB7-based PSC device. These high results indicated that DTBDT should be a promising candidate building block for highly efficient photovoltaic materials.

From the photovoltaic results listed in Table 5.7, BDT and its analogues have been shown to be the most successful building block for highly efficient photovoltaic polymers over 7 %. Notably, the photovoltaic performance of BDT-based polymers such as PTB7, PBDTTT-C-T, and PBDT-DTNT was further increased to 9 % by several groups via device innovations [2–8]. These device optimizations are not presented in this chapter in detail.

5.2.2.6 Thienopyrroledione (TPD)-Based Polymers

The thieno[3,4-*c*]pyrrole-4,6-dione (TPD) family of conjugated polymers has shown promise for PSC applications (see Fig. 5.15 and Table 5.8). The advantage of TPD is relatively cheap and easy synthesis. Incorporation of appropriate alkyl chains on TPD not only enables the preparation of soluble polymers but also greatly tunes the molecular packing as well as blend morphology. TPD-based push-pull polymers for photovoltaic applications were proposed in 2010 by Leclerc and co-workers [145, 146].

In the search for novel polymers suitable for PSCs, Leclerc [146], Jen [147], Xie [148], and Frechet [149] independently synthesized PBDTTPD, which included the benzodithiophene (BDT) unit as donor moiety and TPD as acceptor moiety. The preliminary *PCE* of the PBDTTPD/$PC_{71}BM$-based PSC device was as high as 5.5 % without additive optimization [146]. After utilizing coadditives of chloronaphthalene (CN) and diiodooctane (DIO), a *PCE* up to 7.1 % was achieved by Tao and coworkers [150]. Very recently, alkyl chain engineering was successfully utilized in PBDT-TPD, which dramatically promoted the efficiency of PBDT-TPD by Frechet and coworkers [151]. In their work, replacing branched side chains by linear ones in the

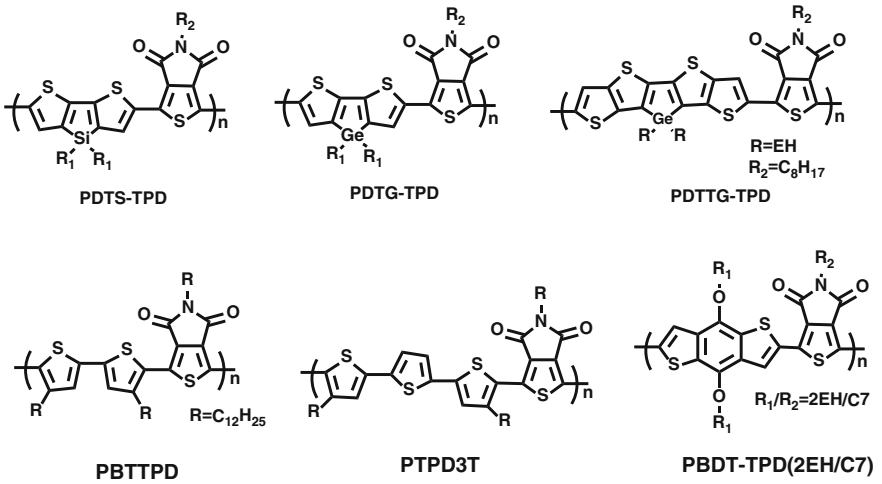

Fig. 5.15 Molecular structures of TPD-based highly efficient polymers

Table 5.8 Photovoltaic performance of the representative D–A copolymers based on BDT analogues

Materials	V_{oc} (V)	J_{sc} (mA/cm^2)	FF (%)	PCE (%)	μ_h [cm^2/(Vs)]	Ref.
PDTS-TPD	0.88	12.2	68	7.3	1×10^{-4}	[94]
PBDT-TPD	0.97	12.6	70	8.5	–	[151]
PDTG-TPD	0.85	12.6	68	7.3	–	[152]
PDTTG-TPD	0.81	13.85	64	7.2	–	[154]
PBTTPD	0.92	13.1	61	7.3	–	[155]
PTPD3T	0.80	12.5	79.6	7.9	1.2×10^{-3}	[157]

BDT motifs induced a critical change in polymer self-assembly and backbone orientation in thin films which correlates with a dramatic drop in solar cell efficiency. In contrast, for polymers with branched alkyl-substituted BDT motifs, controlling the number of carbon atoms in the linear alkyl-substituted TPD motifs could effectively improve material performance. Optimized through this approach, PBDTTPD polymer-based PSC devices acquired high *PCE* of 8.5 % and high V_{oc} of 0.97 V, making PBDTTPD one of the best polymer candidates for the wide band gap subcell of tandem PSCs. This report emphasized the determining role that linear side-chain substituents play in the device performance of PBDTTPD.

In the previous part, a TPD-silole copolymer, PDTS-TPD with high *PCE* up to 7 %, was introduced [94]. In order to improve the intermolecular interactions of silole-based polymers further, Reynolds and co-workers [152] substituted silicon by the larger germanium atom and prepared the first dithienogermole (DTG)-containing conjugated polymer. The dithienogermole-thienopyrrolodione copolymer,

PDTG-TPD, displayed an absorption shift to 735 nm, and a higher HOMO level than the analogous copolymer containing the commonly utilized DTS heterocycle. When PDTG-TPD was utilized in inverted PSCs, the cells displayed an average *PCE* of 7.3 %, relative to 6.6 % for the DTS-containing PSCs prepared under identical conditions. Notably, Reynolds et al. [153] also fabricated highly efficient PSC devices based on PDTG-TPD with a certified *PCE* up to 7.4 %, which is among the highest *PCE*s reported for photovoltaic polymers compatible with the roll-to-roll process. Followed by PDTS-TPD and PDTG-TPD, dithienogermolodithiophene (DTTG) was also incorporated as building blocks in TPD-based polymers because of the potentials of extended conjugation length and improved coplanarity. Very recently, Heeney et al. [154] reported the first synthesis of a novel ladder-type fused ring donor, DTG, in which two thieno[3,2-*b*]thiophene units are held coplanar by a bridging dialkyl germanium (Ge). Polymerization of DTTG with TPD afforded a polymer, PDTTG-TPD, with an optical band gap of 1.75 eV combined with a HOMO level of −5.68 eV. Bulk heterojunction PSC devices based on PDTTG-TPD/$PC_{71}BM$ afforded a *PCE* up to 7.2 % without the need for thermal annealing or processing additives. The preliminary results indicated that DTTG-based polymers are promising candidates for high-performance PSC devices. It should also be noted that the synthetic route provides considerable synthetic scope to promote the performance further by altering the bridging atoms.

Another interesting example of TPD-based copolymer was published by Wei and co-workers [155]. Wei et al. designed a crystalline polymer PDTTPD, which was constructed by bithiophene and TPD. A preliminary *PCE* of 5.0 % (V_{oc} = 0.94 V, J_{sc} = 9.1 mA/cm^2) was achieved for the PBTTPD/$PC_{71}BM$ system. Incorporating a small amount of diiodohexane (DIH) in the blend resulted in the formation of substantially enhanced polymer crystallinity and smaller as well as better dispersed $PC_{71}BM$ domains. As anticipated, an improved J_{sc} as high as 12.1 mA/cm^2 and a *PCE* of 7.3 % were recorded. Following the work of Wei et al., Marks and co-workers [156, 157] developed a series of TPD copolymers bearing thiophene, bithiophene, terthiophene, and quaterthiophene derivatives, respectively, as electron-donating moieties. Among these, a high-performance polymer PTPD3T [157] exhibited a high *PCE* of 7.9 % and extremely high *FF* up to 79.6 %. It is important to emphasize that the synthesis of monomers and polymers is both easy and versatile, wheres that of DTS or DTG derivatives is not.

5.2.2.7 Other Highly Efficient Polymers

As shown in Fig. 5.16 and Table 5.9, besides the above-mentioned polymers, other efficient polymers based on monomers such as quinoxaline (QX), thiazolo[5,4-*d*] thiazole (TTZ), thiophene bridged 2,1,3-benzothiadiazole, or naphtho[1,2-*c*:5,6-*c*] bis [1, 2, 5] thiadiazole also exhibited a high *PCE* over 6 %. QX has been widely implemented as an electron-deficient monomer of LBG polymers in PSCs. In 2010, Wang et al. [158] developed an easily synthesized donor–acceptor polymer (TQ-1) which showed *PCE* up to 6 %, with a high V_{oc} of 0.89 V, indicating that this

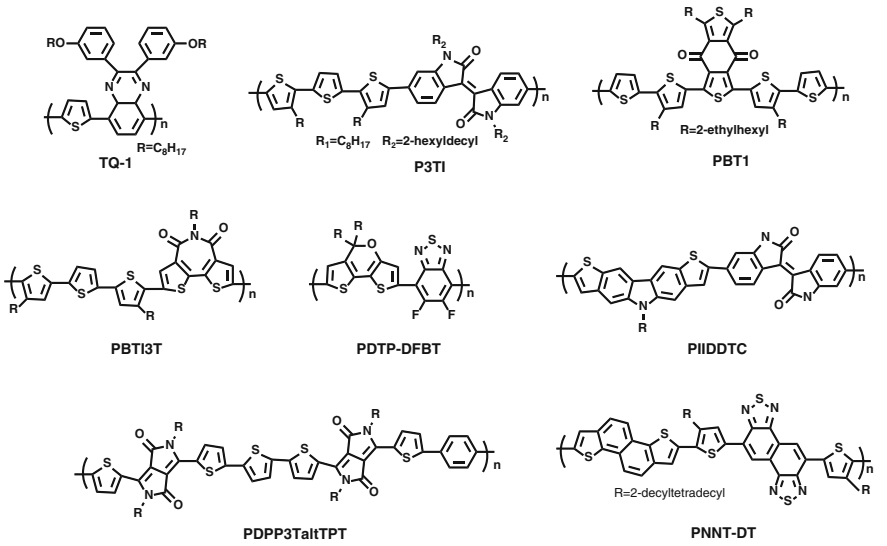

Fig. 5.16 Molecular structures of other highly efficient polymers with *PCE* over 6 %

Table 5.9 The photovoltaic parameters of other highly efficient polymers with *PCE* over 6 %

Materials	V_{oc} (V)	J_{sc} (mA/cm^2)	FF (%)	PCE (%)	μ_h [cm^2/(Vs)]	Ref.
TQ-1	0.89	10.5	64	6.0	–	[158]
P3TI	0.70	13.1	69	6.3	–	[159]
PBT-1	0.83	11.57	71	6.88	–	[160]
PIIDDTC	0.78	15.2	69	8.2	4.9×10^{-4}	[161]
PNNT-BT	0.82	15.6	64	8.2	1.7×10^{-3}	[162]
PDPP3TaltTPT	0.75	15.9	67	8.0	–	[163]
PBTI3T	0.86	12.9	77.8	8.66	1.5×10^{-3}	[153]
PDTP-DFBT	0.70	18.0	63	8.0	3×10^{-3}	[164]

polymer is a particularly promising candidate for high-efficiency low-cost polymer solar cells. Similar to DPP, isoindigo (IID) is also a high-performance pigment, which was developed in recent years for constructing LBG (<1.5 eV) conjugated polymers because of its strong electron-withdrawing character. By choosing the appropriate electron-rich unit terthiophene as the donor and IID as the acceptor, an easily accessible IID-based high-performance photovoltaic polymer (P3TI) was also reported by Wang and coworkers [159]. P3TI/$PC_{71}BM$-based PSC devices have an *IQE* of ~ 87 % and a V_{oc} of 0.7 V with an optimized device *PCE* up to 6.3 %. Qian et al. [160] designed a novel polymer, PBT1, which is copolymerized with benzodithiophene-4,8-dione (BDD) and α-quaterthiophene units. Interestingly, a *PCE* up to 6.88 % was recorded in a PBT1-based PSC under optimal condition of high donor:acceptor ratio (1.5:1, wt:wt) and small thickness (75 nm). This work provided a successful example of using molecular structure as a tool to realize optimal

photovoltaic performance with high polymer content, thereby enabling the realization of efficient absorption in thin films.

A recent breakthrough in several building units was made. Geng and coworkers [161] designed a five-ring-fused aromatic unit, namely dithieno[3,2-*b*;6,7-*b*]carbazole (DTC), which is structurally related to FL. Optimized by inverted device structures, PIIDDTC achieved an extremely high *PCE* of 8.2 %. Notably, PIIDDTC is the first IID-based polymer with a *PCE* beyond 7 %, and amorphous polymer with a *PCE* beyond 8 %. Naphthodithiophene (NDT) also emerged as an efficient building block in highly efficient photovoltaic polymers. Osaka et al. [162] recently developed photovoltaic copolymers based on naphthodithiophene (NDT). Introducing linear alkyl chains improved the solubility as well as gave rise to a change in the orientation without any alteration of the energy levels, which resulted in quite an impressive *PCE* over 8 % in a conventional single-junction PSC device. Surprisingly, the introduction of linear alkyl chains led to a drastic change in polymer orientation into the face-on motif, which was beneficial for the charge transport in solar cells and promotion of the photovoltaic performance. In addition, PSC devices based on the NNT-BT yielded *PCE*s as high as 8.2 % with thickness up to 300 nm. These results indicated that this polymer platform is of particular interest in the understanding of molecular packing and carrier transport in high-performance photoelectronic polymers.

A regular alternating terpolymer design strategy was proposed and applied to produce a photovoltaic polymer with tailored energy levels and optical band gap by Janssen and collaborators [163]. High-molecular-weight photovoltaic materials the terpolymer PDPP3TaltDPP were obtained with high efficiencies up to 8.0 % in PSCs employing $PC_{71}BM$ as acceptors. Relative to the *PCE* of control copolymers PDPP3T (7.1 %) and PDPPTPT (7.4 %), the *PCE* of PDPP3TaltTPT exhibited more than 5 % improvement, which demonstrated that terpolymer could outperform the two parent copolymers when the design strategy was applied.

Similar to PTPD3T, Facchetti [26, 170] also developed a high-performance polymer PBTI3T, which demonstrated excellent *PCE* over 8.6 % and exceptionally high *FF* approaching 80 %. The high *FF* of PBTI3T is comparable to that of their inorganic counterparts. The extremely high *FFs* originated from the highly ordered, closely packed, and properly oriented active-layer microstructures with optimal horizontal phase separation and vertical phase gradation, which is beneficial for efficient charge collection and eliminated bulk as well as interfacial bimolecular recombination. This work depicted a comprehensive example to produce high *FF* in PSC device by integrating complementary materials design, synthesis, processing, and device engineering strategies.

Recently, a dithieno[3,2-*b*:2′,3′-*d*]pyran (DTPy)-containing polymer, PDTP-DFBT, was reported by Yang and coworkers [164]. The electron-donating property of the DTPy unit was found to be the strongest among the most frequently used donor units such as benzodithiophene (BDT) or cyclopentadithiophene (CPDT) units. When DTPy unit was polymerized with the strongly electron-deficient difluorobenzothiadiazole (DFBT) unit, a LBG (E_g = 1.38 eV) polymer PDTP-DFBT was obtained. In comparison with BDT or CPDT units, the DTP-based polymer

PDTP-DFBT showed significantly improved solubility and processability as well as *PCE*. Excellent performance in single and double junction solar cells was obtained with the *PCEs* reaching 8.0 and 10.6 %, respectively, which demonstrated that DTPy unit is a promising building block for high-performance photovoltaic materials.

5.3 Conjugated Polymer Acceptor Materials

Although fullerene acceptors, particularly the well-known PCBM, bis-PCBM, and ICBA have been widely used and performed well with photovoltaic donor polymers in BHJ PSC devices, these materials are still not the best choices for photovoltaic industry due to the high cost and narrow absorption coverage [165]. Because of the high absorption coefficient, broader absorption, and high electron mobilities as well as suitable affinities, non-fullerene acceptors such as perylene bisimide small molecules [166–168], as well as polymers [169, 170], have attracted substantial interest as alternative acceptor materials to fullerene acceptors.

LBG conjugated polymers can also be used as an acceptor in a PSC if its LUMO energy level is low enough. As an electron-deficient building block, PDI can be copolymerized easily with a wide variety of electron-rich units to tailor the molecular levels as well as absorption properties of the resulting D–A copolymers. The molecular structures and photovoltaic results of all-polymer solar cells with *PCE* over 1 % are summarized in Table 5.10 and Fig. 5.17. In 2007, Zhan et al. [171] reported the synthesis of the first soluble rylene containing polymer based on alternating perylene diimide (PDI) and dithienothiophene (DTT), which exhibited good solution processability, broad absorption, excellent thermal stability, and high electron affinity. Electron mobilities as high as 1.3×10^{-2} cm^2 V^{-1} s^{-1} have been measured by the OFET method. All-polymer solar cells using this polymer as acceptor polymer and a polythiophene derivative as donor polymer achieved a high *PCE* of over 1 % under AM 1.5G at 100 mW/cm^2. Similarly, a novel D–A copolymer of perylene diimide (PDI) and dithienothiophene, PPDIDTT-2, was also

Table 5.10 The photovoltaic results of representative acceptor polymer-based PSC devices

Acceptors	Donors	V_{oc} (V)	J_{sc} (mA/cm^2)	FF (%)	PCE (%)	Ref.
PPDIDTT	PT-1	0.63	4.2	39	1.03	[171]
PPDIDTT	PBDTTT-C-T	0.75	8.55	51.5	3.45	[180]
PPDIDTT-2	PT-2	0.69	5.02	43	1.48	[173]
PC-PDI	PT-2	0.70	6.35	50	2.23	[174]
F8TBT	P3HT	1.1	4.0	41	1.8	[176]
P(NDI2OD-T2)	PTB7	0.62	3.4	39	1.1	[178]
N2200	PTQ-1	0.84	8.40	56.0	4.00	[182]
PC-NDI	PTB7	0.88	4.07	38.0	1.34	[181]
PC-NDI	TTV7	0.88	7.71	54.0	3.68	[181]
PNDIT	PSEHTT	0.61	3.80	56	1.30	[179]
PNDIS-HD	PSEHTT	0.76	7.78	55	3.26	[179]

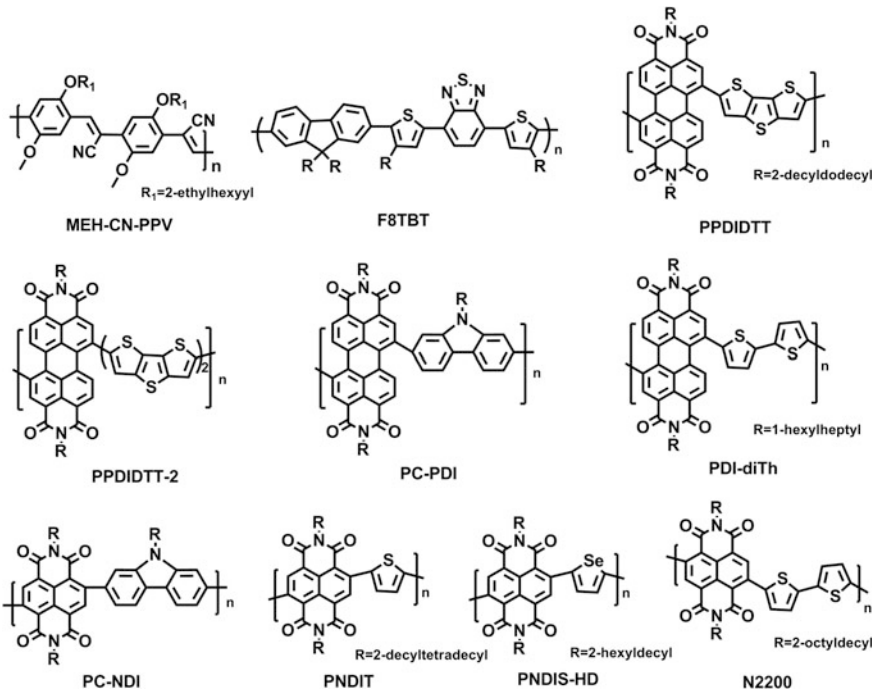

Fig. 5.17 Typical examples of highly efficient acceptor polymers with *PCE* over 1 %

synthesized by Zhan et al. [172], showing a LBG of 1.46 eV and high electron affinity with a LUMO level of 3.9 eV. The copolymer exhibited broad absorption throughout the visible and into the near-IR region. All PSCs were fabricated with the blend PPDIDTT-2 as acceptor and PT-2 as donor (1:1 wt/wt), showing a *PCE* over 1 %. Soon after, Tan et al. [173] optimized the all-polymer solar cells based on the narrow band gap alternating copolymer of perylene diimide and bis(dithienothiophene) (PPDIDTT-2). In their work, a polythiophene derivative substituted by a tris(thienylenevinylene) conjugated side chain (PT-2) are used as donor polymer. The optimized device based on the blend of PT-2 and PPDIDTT-2 in the ratio 3:1 (wt/wt) achieved a J_{sc} of 5.02mA cm^{-2} and a *PCE* of 1.48 %, under AM 1.5 G illumination at 100mW cm^{-2}. In 2010, Zhou et al. [174] systematically investigated all-polymer solar cells based on six perylene diimide-containing polymers (PX-PDI) as acceptor polymers and two polythiophene derivatives (P3HT and PT-2) as donor polymers. The highest *PCE* of 2.23 % was obtained in all-PSCs. The photovoltaic results also depicted that the PSC devices based on the PT1/PX-PDI systems have higher V_{oc} (0.58–0.76 V) than those of the devices based on the P3HT/PX-PDI blends (0.44–0.58 V). Owing to the application of solvent mixtures (toluene/CF, 9:1), the highest *PCE* of all-PSCs based on PT-2/PC-PDI reached 2.23 % because of the optimal phase separation. This work demonstrated that the solvent strategy and two-dimensional conjugated polymer donors are two effective

methods to promote the performance of all-polymer solar cells. Pei et al. [175] developed two perylene diimide (PDI)-based acceptor polymers, r-PDI-diTh and i-PDI-diTh, which were synthesized by introducing a bulky side chain and thereby suppressing the π–π interactions between PDI units in the backbones of acceptor polymers. Therefore, more effective phase segregation of these acceptors with P3HT was realized. When regio-random polymer i-PDI-diTh was blended with P3HT, the PSC device gave a low *PCE* of 0.45 %. By using a similarly structured but regioregular polymer, r-PDI-diTh, the *PCE* further increased to 0.94 % because of the limited defect. By employing the inverted device configuration to match the vertical phase separation of donor polymer/acceptor polymer system better, a desirable *PCE* up to 2.17 % was achieved from the regioregular acceptor polymer, r-PDI-diTh-based PSC devices.

In 2007, McNeill and coworkers [176] reported efficient photovoltaic diodes which used ambipolar poly((9,9-dioctylfluorene)-2,7-diyl-*alt*-[4,7-bis(3-hexylthien-5-yl) -2,1,3-benzothiadiazole]-2′,2″-diyl) (F8TBT) both as acceptor polymer blending with P3HT and as donor polymer blending with $PC_{61}BM$. In both cases, external quantum efficiencies of over 25 % were achieved. In particular, a *PCE* up to 1.8 % and extremely high V_{oc} over 1 V were recorded for the optimized F8TBT/P3HT-based PSC device. Further studies by McNeill et al. [177] demonstrated that the relatively low efficiency of the P3HT/F8BT system can be attributed to poor charge generation and separation efficiencies which result from the failure of P3HT reorganization.

McNeill et al. [178] recently applied PTB7 as the donor polymer in the all-polymer solar cells. A relatively low efficiency of 1.1 % was observed. Clearly, the lack of suitable acceptor polymers has limited the photocurrent and efficiency of polymer/polymer bulk heterojunction solar cells. To overcome the problem, Jenekhe et al. [179] evaluated three naphthalene diimide (NDI) copolymers as acceptor materials in BHJ solar cells. Relatively poor performance ($\sim$1.3 %) was observed in the NDI and thiophene copolymer, PNDIT based all-polymer solar cells. PSCs based on an NDI-selenophene copolymer (PNDIS-HD) acceptor and a thiazolothiazole copolymer (PSEHTT) donor exhibited a high *PCE* of 3.3 %. The observed *FF* values of 55–60 % were impressively high among all-polymer solar cells and comparable to typical values observed in polymer/PCBM systems. Amazingly, this efficiency was comparable to the performance of PSEHTT/PCBM-based PSC devices. The lamellar crystalline morphology of PNDIS-HD, leading to balanced electron and hole transport in the polymer/polymer blend solar cells, should account for the good performance.

Cheng et al. [180] recently introduced two-dimensional polymer PBDTTT-C-T as donor polymer and proposed a binary additive approach to optimize the performance of PPDIDTT-based all-polymer solar cells, and a dramatically improved *PCE* up to 3.45 % was observed. Zhou et al. [181] recently reported a high *PCE* of 3.68 % for the all-polymer solar cell utilizing TTV as the donor polymer and PC-NDI as the acceptor polymer. By introducing a conjugated side chain in the TT unit of donor polymer PTB7, the miscibility of the polymer/polymer blend was greatly improved. In addition, adding a small amount (1 vol.%) of 1,8-diiodooctane (DIO)

could increase the aggregation of acceptor polymer, PC-NDI. For the PTB7/PC-NDI-based all-PSCs, the *PCE* decreased to 1.12 % with V_{oc} = 0.86 V, J_{sc} = 3.83 mA/cm^2, and *FF* = 34 %. This work demonstrated that two-dimensional conjugated polymer might be ideal donor polymers for all-polymer solar cells because of the superior properties. More recently, Mori et al. [182] fabricated highly efficient LBG donor/acceptor polymer blend solar cells by utilizing TQ-1 as donor polymer and N2200 as acceptor polymer. The device performance was optimized at a donor/acceptor blending ratio of 7:3 (wt:wt) to result in a high J_{sc} of 8.85 mA/cm^2, a *FF* of 55 %, and a V_{oc} of 0.84 V. The high *PCE* exceeded 4 %, which was among the highest values reported for all-polymer solar cells. The high photovoltaic performance demonstrated the great potential of polymer/polymer blend solar cells as a promising alternative to polymer/fullerene solar cells.

Because the typical exciton diffusion length of polymer/polymer blends is approximately 10 nm, the larger phase separation length and smaller donor/acceptor interfacial area in the polymer/polymer systems might be the origin of inefficient exciton dissociation and relatively low performance in these systems. To improve the performance of all-polymer solar cells, two strategies could be utilized. One strategy is morphology tuning, for instance, altering the processing solvent to modulate the scale and degree of phase separation of D/A blends. The other strategy is to rationally select and design superior donor polymers.

5.4 Summary and Outlook

In this chapter, an overview of conjugated polymer photovoltaic materials developed during the past two decades are summarized and commented. The basic design considerations of the conjugated polymer photovoltaic materials for the application in polymer solar cells are also discussed along with examples. The rapid progress in novel conjugated photovoltaic polymers demonstrates that there is plenty of room to bring the cost of PSCs down by developing low-cost and highly efficient polymeric photovoltaic materials [183, 184]. Guided by computational calculations and screening [185], further improvements will be realized in the near future by fine optimization of integrated backbones, side chains, and molecular weight [186] based on well-defined highly efficient polymers.

References

1. Li XH, Choy WCH, Huo LJ, Xie FX, Sha WEI, Ding BF, Guo X, Li YF, Hou JH, You JB, Yang Y (2012) Dual plasmonic nanostructures for high performance inverted organic solar cells. Adv Mater 24:3046–3052
2. Chang C-Y, Zuo L, Yip H-L, Li Y, Li C-Z, Hsu C-S, Cheng Y-J, Chen H, Jen AKY (2013) A versatile fluoro-containing low-bandgap polymer for efficient semitransparent and tandem polymer solar cells. Adv Funct Mater 23:5084–5090

3. Liu S, Zhang K, Lu J, Zhang J, Yip H-L, Huang F, Cao Y (2013) High-efficiency polymer solar cells via the incorporation of an amino-functionalized conjugated metallopolymer as a cathode interlayer. J Am Chem Soc 135:15326–15329
4. Yang TB, Wang M, Duan CH, Hu XW, Huang L, Peng JB, Huang F, Gong X (2012) Inverted polymer solar cells with 8.4 % efficiency by conjugated polyelectrolyte. Energy Environ Sci 5:8208–8214
5. Tan Z, Li L, Wang F, Xu Q, Li S, Sun G, Tu X, Hou X, Hou J, Li Y (2014) Solution-processed rhenium oxide: A versatile anode buffer layer for high performance polymer solar cells with enhanced light harvest. Adv Energy Mater 4. doi:10.1002/aenm.201300884
6. Duan CH, Zhang K, Guan X, Zhong CM, Xie HM, Huang F, Chen JW, Peng JB, Cao Y (2013) Conjugated zwitterionic polyelectrolyte-based interface modification materials for high performance polymer optoelectronic devices. Chem Sci 4:1298–1307
7. He ZC, Zhong CM, Huang X, Wong WY, Wu HB, Chen LW, Su SJ, Cao Y (2011) Simultaneous enhancement of open-circuit voltage, short-circuit current density, and fill factor in polymer solar cells. Adv Mater 23:4636–4643
8. He ZC, Zhong CM, Su SJ, Xu M, Wu HB, Cao Y (2012) Enhanced power-conversion efficiency in polymer solar cells using an inverted device structure. Nat Photonics 6:591–595
9. Dou LT, You JB, Yang J, Chen CC, He YJ, Murase S, Moriarty T, Emery K, Li G, Yang Y (2012) Tandem polymer solar cells featuring a spectrally matched low-bandgap polymer. Nat Photonics 6:180–185
10. Dou LT, Chang WH, Gao J, Chen CC, You JB, Yang Y (2013) A selenium-substituted low-bandgap polymer with versatile photovoltaic applications. Adv Mater 25:825–831
11. Dou LT, Gao J, Richard E, You JB, Chen CC, Cha KC, He YJ, Li G, Yang Y (2012) Systematic investigation of benzodithiophene- and diketopyrrolopyrrole-based low-bandgap polymers designed for single junction and tandem polymer solar cells. J Am Chem Soc 134:10071–10079
12. Liao S-H, Jhuo H-J, Cheng Y-S, Chen S-A (2013) Fullerene derivative-doped zinc oxide nanofilm as the cathode of inverted polymer solar cells with low-bandgap polymer (PTB7-Th) for high performance. Adv Mater 25:4766–4771
13. You J, Dou L, Yoshimura K, Kato T, Ohya K, Moriarty T, Emery K, Chen C-C, Gao J, Li G, Yang Y (2013) A polymer tandem solar cell with 10.6 % power conversion efficiency. Nat Commun 4:1446
14. Yu G, Gao J, Hummelen JC, Wudl F, Heeger AJ (1995) Polymer photovoltaic cells—enhanced efficiencies via a network of internal donor–acceptor heterojunctions. Science 270:1789–1791
15. Halls JJM, Walsh CA, Greenham NC, Marseglia EA, Friend RH, Moratti SC, Holmes AB (1995) Efficient photodiodes from interpenetrating polymer networks. Nature 376:498–500
16. Li YF, Zou YP (2008) Conjugated polymer photovoltaic materials with broad absorption band and high charge carrier mobility. Adv Mater 20:2952–2958
17. Cheng YJ, Yang SH, Hsu CS (2009) Synthesis of conjugated polymers for organic solar cell applications. Chem Rev 109:5868–5923
18. Chen J, Cao Y (2009) Development of novel conjugated donor polymers for high-efficiency bulk-heterojunction photovoltaic devices. Acc Chem Res 42:1709–1718
19. Beaujuge PM, Fréchet JMJ (2011) Molecular design and ordering effects in π-functional materials for transistor and solar cell applications. J Am Chem Soc 133:20009–20029
20. He F, Yu LP (2011) How far can polymer solar cells go? In need of a synergistic approach. J Phys Chem Lett 2:3102–3113
21. Li YF (2012) Molecular design of photovoltaic materials for polymer solar cells: toward suitable electronic energy levels and broad absorption. Acc Chem Res 45:723–733
22. Ye L, Zhang SQ, Huo LJ, Zhang MJ, Hou JH (2014) Molecular design toward highly efficient photovoltaic polymers based on two-Dimensional conjugated benzodithiophene. Acc Chem Res 47:1595–1603
23. Zhou HX, Yang LQ, You W (2012) Rational design of high performance conjugated polymers for organic solar cells. Macromolecules 45:607–632

24. Henson ZB, Mullen K, Bazan GC (2012) Design strategies for organic semiconductors beyond the molecular formula. Nat Chem 4:699–704
25. Son HJ, Carsten B, Jung IH, Yu LP (2012) Overcoming efficiency challenges in organic solar cells: rational development of conjugated polymers. Energy Environ Sci 5:8158–8170
26. Facchetti A (2011) pi-conjugated polymers for organic electronics and photovoltaic cell applications. Chem Mater 23:733–758
27. Spanggaard H, Krebs FC (2004) A brief history of the development of organic and polymeric photovoltaics. Sol Energy Mater Sol C 83:125–146
28. Liang YY, Yu LP (2010) A new class of semiconducting polymers for bulk heterojunction solar cells with exceptionally high performance. Acc Chem Res 43:1227–1236
29. Zhan XW, Zhu DB (2010) Conjugated polymers for high-efficiency organic photovoltaics. Polym Chem 1:409–419
30. Helgesen M, Sondergaard R, Krebs FC (2010) Advanced materials and processes for polymer solar cell devices. J Mater Chem 20:36–60
31. Scharber MC, Wuhlbacher D, Koppe M, Denk P, Waldauf C, Heeger AJ, Brabec CL (2006) Design rules for donors in bulk-heterojunction solar cells—towards 10 % energy-conversion efficiency. Adv Mater 18:789–794
32. Liu F, Gu Y, Shen X, Ferdous S, Wang H-W, Russell TP (2013) Characterization of the morphology of solution-processed bulk heterojunction organic photovoltaics. Prog Polym Sci 38:1990–2052
33. Ye L, Jing Y, Guo X, Sun H, Zhang S, Zhang M, Huo L, Hou J (2013) Remove the residual additives toward enhanced efficiency with higher reproducibility in polymer solar cells. J Phys Chem C 117:14920–14928
34. Bijleveld JC, Zoombelt AP, Mathijssen SGJ, Wienk MM, Turbiez M, de Leeuw DM, Janssen RAJ (2009) Poly(diketopyrrolopyrrole-terthiophene) for ambipolar logic and photovoltaics. J Am Chem Soc 131:16616–16617
35. Ye L, Zhang S, Ma W, Fan B, Guo X, Huang Y, Ade H, Hou J (2012) From binary to ternary solvent: morphology fine-tuning of D/A blends in PDPP3T-based polymer solar cells. Adv Mater 24:6335–6341
36. Wessling RA (1985) The polymerization of xylylene bisdialkyl sulfonium salts. J Polym Sci Polym Symp 72:55–66
37. Gilch HG, Wheelwright WL (1966) Polymerization of α-halogenated p-xylenes with base. J Polym Sci A-1: Polym Chem 4:1337–1349
38. Hou J, Fan B, Huo L, He C, Yang C, Li Y (2006) Poly(alkylthio-p-phenylenevinylene): synthesis and electroluminescent and photovoltaic properties. J Polym Sci A: Polym Chem 44:1279–1290
39. Namazi H, Assadpour A, Pourabbas B, Entezami A (2001) Polycondensation of bis (cyanoacetate) and a,10bdihydrobenzofuro[2,3-b]benzofuran-2,9-dicarbaldehyde via knoevenagel reaction: synthesis of donor–acceptor polymers containing shoulder-to-shoulder main chains. J Appl Polym Sci 81:505–511
40. Shaheen SE, Brabec CJ, Sariciftci NS, Padinger F, Fromherz T, Hummelen JC (2001) 2.5 % efficient organic plastic solar cells. Appl Phys Lett 78:841–843
41. Brabec CJ, Shaheen SE, Winder C, Sariciftci NS, Denk P (2002) Effect of LiF/metal electrodes on the performance of plastic solar cells. Appl Phys Lett 80:1288–1290
42. Zhou QM, Zheng LP, Sun DK, Deng XY, Yu G, Cao Y (2003) Efficient polymer photovoltaic devices based on blend of MEH-PPV and C-60 derivatives. Synth Met 135:825–826
43. Wienk MM, Kroon JM, Verhees WJH, Knol J, Hummelen JC, van Hal PA, Janssen RAJ (2003) Efficient methano[70]fullerene/MDMO-PPV bulk heterojunction photovoltaic cells. Angew Chem Int Ed 42:3371–3375
44. Tajima K, Suzuki Y, Hashimoto K (2008) Polymer photovoltaic devices using fully regioregular poly[(2-methoxy-5-(3′,7′-dimethyloctyloxy))-1,4-phenylenevinylene]. J Phys Chem C 112:8507–8510

45. Mikroyannidis JA, Kabanakis AN, Balraju P, Sharma GD (2010) Enhanced performance of bulk heterojunction solar cells using novel alternating phenylenevinylene copolymers of low band gap with cyanovinylene 4-nitrophenyls. Macromolecules 43:5544–5553
46. Hou JH, Tan Z, He YJ, Yang CH, Li YF (2006) Branched poly(thienylene vinylene)s with absorption spectra covering the whole visible region. Macromolecules 39:4657–4662
47. Huo LJ, Chen TL, Zhou Y, Hou JH, Chen HY, Yang Y, Li YF (2009) Improvement of photoluminescent and photovoltaic properties of poly(thienylene vinylene) by carboxylate substitution. Macromolecules 42:4377–4380
48. He Y, Zhou Y, Zhao G, Min J, Guo X, Zhang B, Zhang M, Zhang J, Li Y, Zhang F, Inganäs O (2010) Poly(4,8-bis(2-ethylhexyloxy)benzo[1,2-b:4,5-b′]dithiophene vinylene): synthesis, optical and photovoltaic properties. J Polym Sci A: Polym Chem 48:1822–1829
49. Sato M, Morii H (1991) Configurational feature of electrochemically-prepared poly(3-dodecylthiophene). Polym Commun 32:42–44
50. McCullough RD (1998) The chemistry of conducting polythiophenes. Adv Mater 10:93–116
51. Sugimoto R, Takeda S, Gu HB, Yoshino K (1986) Preparation of soluble polythiophene derivatives utilizing transition metal halides as catalysts and their property. Chem Express 1:635–638
52. Pomerantz M, Tseng JJ, Zhu H, Sproull SJ, Reynolds JR, Uitz R, Arnott HJ, Haider MI (1991) Processable polymers and copolymers of 3-alkylthiophenes and their blends. Synth Met 41:825–830
53. Mccullough RD, Lowe RD (1992) Enhanced electrical-conductivity in regioselectively synthesized poly(3-alkylthiophenes). J Chem Soc Chem Comm 1:70–72
54. Chen TA, Rieke RD (1993) Polyalkylthiophenes with the smallest bandgap and the highest intrinsic conductivity. Synth Met 60:175–177
55. Iraqi A, Barker GW (1998) Synthesis and characterisation of telechelic regioregular head-to-tail poly(3-alkylthiophenes). J Mater Chem 8:25–29
56. Guillerez S, Bidan G (1998) New convenient synthesis of highly regioregular poly (3-octylthiophene) based on the Suzuki coupling reaction. Synth Met 93:123–126
57. Brabec CJ (2004) Organic photovoltaics: technology and market. Sol Energy Mat Sol C 83:273–292
58. Dang MT, Hirsch L, Wantz G (2011) P3HT:PCBM, best seller in polymer photovoltaic research. Adv Mater 23:3597–3602
59. Dang MT, Hirsch L, Wantz G, Wuest JD (2013) Controlling the morphology and performance of bulk heterojunctions in solar cells. Lessons learned from the benchmark poly (3-hexylthiophene):[6, 6]-phenyl-C_{61}-butyric acid methyl ester system. Chem Rev 113:3734–3765
60. Padinger F, Rittberger RS, Sariciftci NS (2003) Effects of postproduction treatment on plastic solar cells. Adv Funct Mater 13:85–88
61. Li G, Shrotriya V, Huang JS, Yao Y, Moriarty T, Emery K, Yang Y (2005) High-efficiency solution processable polymer photovoltaic cells by self-organization of polymer blends. Nat Mater 4:864–868
62. Ma WL, Yang CY, Gong X, Lee K, Heeger AJ (2005) Thermally stable, efficient polymer solar cells with nanoscale control of the interpenetrating network morphology. Adv Funct Mater 15:1617–1622
63. He YJ, Chen HY, Hou JH, Li YF (2010) Indene-C-60 bisadduct: a new acceptor for high-performance polymer solar cells. J Am Chem Soc 132:1377–1382
64. Zhao G, He Y, Li Y (2010) 6.5 % efficiency of polymer solar cells based on poly(3-hexylthiophene) and indene-C_{60} bisadduct by device optimization. Adv Mater 22:4355–4358
65. Guo X, Cui CH, Zhang MJ, Huo LJ, Huang Y, Hou JH, Li Y (2012) High efficiency polymer solar cells based on poly(3-hexylthiophene)/indene-C-70 bisadduct with solvent additive. Energy Environ Sci 5:7943–7949
66. Li G, Yao Y, Yang H, Shrotriya V, Yang G, Yang Y (2007) "Solvent annealing" effect in polymer solar cells based on poly(3-hexylthiophene) and methanofullerenes. Adv Funct Mater 17:1636–1644

67. Yao Y, Hou JH, Xu Z, Li G, Yang Y (2008) Effect of solvent mixture on the nanoscale phase separation in polymer solar cells. Adv Funct Mater 18:1783–1789
68. Nguyen LH, Hoppe H, Erb T, Günes S, Gobsch G, Sariciftci NS (2007) Effects of annealing on the nanomorphology and performance of poly(alkylthiophene): fullerene bulk-heterojunction solar cells. Adv Funct Mater 17:1071–1078
69. Wu PT, Xin H, Kim FS, Ren GQ, Jenekhe SA (2009) Regioregular poly(3-pentylthiophene): synthesis, self-assembly of nanowires, high-mobility field-effect transistors, and efficient photovoltaic cells. Macromolecules 42:8817–8826
70. Xin H, Kim FS, Jenekhe SA (2008) Highly efficient solar cells based on poly (3-butylthiophene) nanowires. J Am Chem Soc 130:5424–5425
71. Gadisa A, Oosterbaan WD, Vandewal K, Bolsée J-C, Bertho S, D'Haen J, Lutsen L, Vanderzande D, Manca JV (2009) Effect of alkyl side-chain length on photovoltaic properties of poly(3-alkylthiophene)/PCBM bulk heterojunctions. Adv Funct Mater 19:3300–3306
72. Sun Y, Cui C, Wang H, Li Y (2012) High-efficiency polymer solar cells based on poly (3-pentylthiophene) with indene-C_{70} bisadduct as an acceptor. Adv Energy Mater 2:966–969
73. Hou JH, Tan ZA, Yan Y, He YJ, Yang CH, Li YF (2006) Synthesis and photovoltaic properties of two-dimensional conjugated polythiophenes with bi(thienylenevinylene) side chains. J Am Chem Soc 128:4911–4916
74. Hou JH, Chen TL, Zhang SQ, Huo LJ, Sista S, Yang Y (2009) An easy and effective method to modulate molecular energy level of poly(3-alkylthiophene) for high-V-oc polymer solar cells. Macromolecules 42:9217–9219
75. Zhang MJ, Guo X, Yang Y, Zhang J, Zhang ZG, Li YF (2011) Downwards tuning the HOMO level of polythiophene by carboxylate substitution for high open-circuit-voltage polymer solar cells. Polym Chem 2:2900–2906
76. Svensson M, Zhang F, Veenstra SC, Verhees WJH, Hummelen JC, Kroon JM, Inganäs O, Andersson MR (2003) High-performance polymer solar cells of an alternating polyfluorene copolymer and a fullerene derivative. Adv Mater 15:988–991
77. Chen MH, Hou J, Hong Z, Yang G, Sista S, Chen LM, Yang Y (2009) Efficient polymer solar cells with thin active layers based on alternating polyfluorene copolymer/fullerene bulk heterojunctions. Adv Mater 21:4238–4242
78. Mühlbacher D, Scharber M, Morana M, Zhu Z, Waller D, Gaudiana R, Brabec C (2006) High photovoltaic performance of a low-bandgap polymer. Adv Mater 18:2884–2889
79. Peet J, Kim JY, Coates NE, Ma WL, Moses D, Heeger AJ, Bazan GC (2007) Efficiency enhancement in low-bandgap polymer solar cells by processing with alkane dithiols. Nat Mater 6:497–500
80. Blouin N, Michaud A, Leclerc M (2007) A low-bandgap poly(2,7-Carbazole) derivative for use in high-performance solar cells. Adv Mater 19:2295–2300
81. Park SH, Roy A, Beaupre S, Cho S, Coates N, Moon JS, Moses D, Leclerc M, Lee K, Heeger AJ (2009) Bulk heterojunction solar cells with internal quantum efficiency approaching 100 %. Nat Photonics 3:297–302
82. Beaupre S, Leclerc M (2013) PCDTBT: en route for low cost plastic solar cells. J Mater Chem A 1:11097–11105
83. Qin RP, Li WW, Li CH, Du C, Veit C, Schleiermacher HF, Andersson M, Bo ZS, Liu ZP, Inganas O, Wuerfel U, Zhang FL (2009) A planar copolymer for high efficiency polymer solar cells. J Am Chem Soc 131:14612–14613
84. Wong WY, Wang XZ, He Z, Djurisic AB, Yip CT, Cheung KY, Wang H, Mak CSK, Chan WK (2007) Metallated conjugated polymers as a new avenue towards high-efficiency polymer solar cells. Nat Mater 6:521–527
85. Wang EG, Wang L, Lan LF, Luo C, Zhuang WL, Peng JB, Cao Y (2008) High-performance polymer heterojunction solar cells of a polysilafluorene derivative. Appl Phys Lett 92:033307
86. Song J, Du C, Li C, Bo Z (2011) Silole-containing polymers for high-efficiency polymer solar cells. J Polym Sci A: Polym Chem 49:4267–4274

87. Hou JH, Chen HY, Zhang SQ, Li G, Yang Y (2008) Synthesis, characterization, and photovoltaic properties of a low band gap polymer based on silole-containing polythiophenes and 2,1,3-benzothiadiazole. J Am Chem Soc 130:16144–16145
88. Chen HY, Hou JH, Hayden AE, Yang H, Houk KN, Yang Y (2010) Silicon atom substitution enhances interchain packing in a thiophene-based polymer system. Adv Mater 22:371–375
89. Scharber MC, Koppe M, Gao J, Cordella F, Loi MA, Denk P, Morana M, Egelhaaf HJ, Forberich K, Dennler G, Gaudiana R, Waller D, Zhu ZG, Shi XB, Brabec CJ (2010) Influence of the bridging atom on the performance of a low-bandgap bulk heterojunction solar cell. Adv Mater 22:367–370
90. Morana M, Azimi H, Dennler G, Egelhaaf H-J, Scharber M, Forberich K, Hauch J, Gaudiana R, Waller D, Zhu Z, Hingerl K, van Bavel SS, Loos J, Brabec CJ (2010) Nanomorphology and charge generation in bulk heterojunctions based on low-bandgap dithiophene polymers with different bridging atoms. Adv Funct Mater 20:1180–1188
91. Zhang M, Guo X, Li Y (2011) Synthesis and characterization of a copolymer based on thiazolothiazole and dithienosilole for polymer solar cells. Adv Energy Mater 1:557–560
92. Cui C, Fan X, Zhang M, Zhang J, Min J, Li Y (2011) A D-A copolymer of dithienosilole and a new acceptor unit of naphtho[2,3-c]thiophene-4,9-dione for efficient polymer solar cells. Chem Commun 47:11345–11347
93. Guo X, Zhou N, Lou SJ, Hennek JW, Ponce Ortiz R, Butler MR, Boudreault P-LT, Strzalka J, Morin P-O, Leclerc M, López Navarrete JT, Ratner MA, Chen LX, Chang RPH, Facchetti A, Marks TJ (2012) Bithiopheneimide–dithienosilole/dithienogermole copolymers for efficient solar cells: information from structure–property–device performance correlations and comparison to thieno[3,4-c]pyrrole-4,6-dione analogues. J Am Chem Soc 134:18427–18439
94. Chu T-Y, Lu J, Beaupré S, Zhang Y, Pouliot J-R, Wakim S, Zhou J, Leclerc M, Li Z, Ding J, Tao Y (2011) Bulk heterojunction solar cells using thieno[3,4-c]pyrrole-4,6-dione and dithieno[3,2-b:2′,3′-d]silole copolymer with a power conversion efficiency of 7.3 %. J Am Chem Soc 133:4250–4253
95. Wienk MM, Turbiez M, Gilot J, Janssen RAJ (2008) Narrow-bandgap diketo-pyrrolo-pyrrole polymer solar cells: the effect of processing on the performance. Adv Mater 20:2556–2560
96. Huo LJ, Hou JH, Chen HY, Zhang SQ, Jiang Y, Chen TL, Yang Y (2009) Bandgap and molecular level control of the low-bandgap polymers based on 3,6-dithiophen-2-yl-2,5-dihydropyrrolo[3,4-c]pyrrole-1,4-dione toward highly efficient polymer solar cells. Macromolecules 42:6564–6571
97. Li W, Furlan A, Hendriks KH, Wienk MM, Janssen RAJ (2013) Efficient tandem and triple-junction polymer solar cells. J Am Chem Soc 135:5529–5532
98. Bronstein H, Chen ZY, Ashraf RS, Zhang WM, Du JP, Durrant JR, Tuladhar PS, Song K, Watkins SE, Geerts Y, Wienk MM, Janssen RAJ, Anthopoulos T, Sirringhaus H, Heeney M, McCulloch I (2011) Thieno[3,2-b]thiophene-diketopyrrolopyrrole-containing polymers for high-performance organic field-effect transistors and organic photovoltaic devices. J Am Chem Soc 133:3272–3275
99. Bronstein H, Collado-Fregoso E, Hadipour A, Soon YW, Huang Z, Dimitrov SD, Ashraf RS, Rand BP, Watkins SE, Tuladhar PS, Meager I, Durrant JR, McCulloch I (2013) Thieno[3,2-b]thiophene-diketopyrrolopyrrole containing polymers for inverted solar cells devices with high short circuit currents. Adv Funct Mater 23:5647–5654
100. Li W, Hendriks KH, Roelofs WSC, Kim Y, Wienk MM, Janssen RAJ (2013) Efficient small bandgap polymer solar cells with high fill factors for 300 nm thick films. Adv Mater 25:3182–3186
101. Bijleveld JC, Gevaerts VS, Di Nuzzo D, Turbiez M, Mathijssen SGJ, de Leeuw DM, Wienk MM, Janssen RAJ (2010) Efficient solar cells based on an easily accessible diketopyrrolopyrrole polymer. Adv Mater 22:E242–E246
102. Yiu AT, Beaujuge PM, Lee OP, Woo CH, Toney MF, Frechet JMJ (2012) Side-chain tunability of furan-containing low-band-gap polymers provides control of structural order in efficient solar cells. J Am Chem Soc 134:2180–2185

103. Woo CH, Beaujuge PM, Holcombe TW, Lee OP, Frechet JMJ (2010) Incorporation of furan into low band-gap polymers for efficient solar cells. J Am Chem Soc 132:15547–15549
104. Li WW, Hendriks KH, Furlan A, Roelofs WSC, Wienk MM, Janssen RAJ (2013) Universal correlation between fibril width and quantum efficiency in diketopyrrolopyrrole-based polymer solar cells. J Am Chem Soc 135:18942–18948
105. Mcculloch I, Ashraf RS, Biniek L, Bronstein H, Combe C, Donaghey JE, James DI, Nielsen CB, Schroeder BC, Zhang WM (2012) Design of semiconducting indacenodithiophene polymers for high performance transistors and solar cells. Acc Chem Res 45:714–722
106. Chen CP, Chan SH, Chao TC, Ting C, Ko BT (2008) Low-bandgap poly(thiophene-phenylene-thiophene) derivatives with broaden absorption spectra for use in high-performance bulk-heterojunction polymer solar cells. J Am Chem Soc 130:12828–12833
107. Yu CY, Chen CP, Chan SH, Hwang GW, Ting C (2009) Thiophene/phenylene/thiophene-based low-bandgap conjugated polymers for efficient near-infrared photovoltaic applications. Chem Mater 21:3262–3269
108. Chen YC, Yu CY, Fan YL, Hung LI, Chen CP, Ting C (2010) Low-bandgap conjugated polymer for high efficient photovoltaic applications. Chem Commun 46:6503–6505
109. Zhang Y, Zou JY, Yip HL, Chen KS, Zeigler DF, Sun Y, Jen AKY (2011) Indacenodithiophene and quinoxaline-based conjugated polymers for highly efficient polymer solar cells. Chem Mater 23:2289–2291
110. Zhang Y, Chien SC, Chen KS, Yip HL, Sun Y, Davies JA, Chen FC, Jen AKY (2011) Increased open circuit voltage in fluorinated benzothiadiazole-based alternating conjugated polymers. Chem Commun 47:11026–11028
111. Xu YX, Chueh CC, Yip HL, Ding FZ, Li YX, Li CZ, Li XS, Chen WC, Jen AKY (2012) Improved charge transport and absorption coefficient in indacenodithieno[3,2-b]thiophene-based ladder-type polymer leading to highly efficient polymer solar cells. Adv Mater 24:6356–6361
112. Wang M, Hu XW, Liu LQ, Duan CH, Liu P, Ying L, Huang F, Cao Y (2013) Design and synthesis of copolymers of indacenodithiophene and naphtho[1,2-c:5,6-c]bis(1,2,5-thiadiazole) for polymer solar cells. Macromolecules 46:3950–3958
113. Zhang MJ, Guo X, Wang XC, Wang HQ, Li YF (2011) Synthesis and photovoltaic properties of D-A copolymers based on alkyl-substituted indacenodithiophene donor unit. Chem Mater 23:4264–4270
114. Intemann JJ, Yao K, Yip HL, Xu YX, Li YX, Liang PW, Ding FZ, Li XS, Jen AKY (2013) Molecular weight effect on the absorption, charge carrier mobility, and photovoltaic performance of an indacenodiselenophene-based ladder-type polymer. Chem Mater 25:3188–3195
115. Guo X, Zhang MJ, Tan JH, Zhang SQ, Huo LJ, Hu WP, Li YF, Hou JH (2012) Influence of D/A ratio on photovoltaic performance of a highly efficient polymer solar cell system. Adv Mater 24:6536–6541
116. Huo LJ, Hou JH (2011) Benzo[1,2-b:4,5-b′]dithiophene-based conjugated polymers: band gap and energy level control and their application in polymer solar cells. Polym Chem 2:2453–2461
117. Hou JH, Park MH, Zhang SQ, Yao Y, Chen LM, Li JH, Yang Y (2008) Bandgap and molecular energy level control of conjugated polymer photovoltaic materials based on benzo [1,2-b : 4,5-b′]dithiophene. Macromolecules 41:6012–6018
118. Liang YY, Wu Y, Feng DQ, Tsai ST, Son HJ, Li G, Yu LP (2009) Development of new semiconducting polymers for high performance solar cells. J Am Chem Soc 131:56–57
119. Liang YY, Feng DQ, Wu Y, Tsai ST, Li G, Ray C, Yu LP (2009) Highly efficient solar cell polymers developed via fine-tuning of structural and electronic properties. J Am Chem Soc 131:7792–7799
120. Liang YY, Xu Z, Xia JB, Tsai ST, Wu Y, Li G, Ray C, Yu LP (2010) For the bright future-bulk heterojunction polymer solar cells with power conversion efficiency of 7.4 %. Adv Mater 22:E135–E138

121. Hou JH, Chen HY, Zhang SQ, Chen RI, Yang Y, Wu Y, Li G (2009) Synthesis of a low band gap polymer and its application in highly efficient polymer solar cells. J Am Chem Soc 131:15586–15587
122. Chen HY, Hou JH, Zhang SQ, Liang YY, Yang GW, Yang Y, Yu LP, Wu Y, Li G (2009) Polymer solar cells with enhanced open-circuit voltage and efficiency. Nat Photonics 3:649–653
123. Huang Y, Huo LJ, Zhang SQ, Guo X, Han CC, Li YF, Hou JH (2011) Sulfonyl: a new application of electron-withdrawing substituent in highly efficient photovoltaic polymer. Chem Commun 47:8904–8906
124. Zhou HX, Yang LQ, Stuart AC, Price SC, Liu SB, You W (2011) Development of fluorinated benzothiadiazole as a structural unit for a polymer solar cell of 7 % efficiency. Angew Chem Int Ed 50:2995–2998
125. Wang N, Chen Z, Wei W, Jiang ZH (2013) Fluorinated benzothiadiazole-based conjugated polymers for high-performance polymer solar cells without any processing additives or post-treatments. J Am Chem Soc 135:17060–17068
126. Price SC, Stuart AC, Yang LQ, Zhou HX, You W (2011) Fluorine substituted conjugated polymer of medium band gap yields 7 % efficiency in polymer-fullerene solar cells. J Am Chem Soc 133:4625–4631
127. Li K, Li Z, Feng K, Xu X, Wang L, Peng Q (2013) Development of large band-gap conjugated copolymers for efficient regular single and tandem organic solar cells. J Am Chem Soc 135:13549–13557
128. Wang XC, Jiang P, Chen Y, Luo H, Zhang ZG, Wang HQ, Li XY, Yu G, Li YF (2013) Thieno[3,2-b]thiophene-bridged D-pi-A polymer semiconductor based on benzo[1,2-b:4,5-b′]dithiophene and benzoxadiazole. Macromolecules 46:4805–4812
129. Chen HC, Chen YH, Liu CC, Chien YC, Chou SW, Chou PT (2012) Prominent short-circuit currents of fluorinated quinoxaline-based copolymer solar cells with a power conversion efficiency of 8.0 %. Chem Mater 24:4766–4772
130. Huo LJ, Hou JH, Zhang SQ, Chen HY, Yang Y (2010) A polybenzo[1,2-b:4,5-b′] dithiophene derivative with deep HOMO level and its application in high-performance polymer solar cells. Angew Chem Int Ed 49:1500–1503
131. Huo LJ, Zhang SQ, Guo X, Xu F, Li YF, Hou JH (2011) Replacing alkoxy groups with alkylthienyl groups: a feasible approach to improve the properties of photovoltaic polymers. Angew Chem Int Ed 50:9697–9702
132. Huang Y, Guo X, Liu F, Huo LJ, Chen YN, Russell TP, Han CC, Li YF, Hou JH (2012) Improving the ordering and photovoltaic properties by extending pi-conjugated area of electron-donating units in polymers with D-A structure. Adv Mater 24:3383–3389
133. Duan RM, Ye L, Guo X, Huang Y, Wang P, Zhang SQ, Zhang JP, Huo LJ, Hou JH (2012) Application of two-dimensional conjugated benzo[1,2-b:4,5-b′]dithiophene in quinoxaline-based photovoltaic polymers. Macromolecules 45:3032–3038
134. Guo X, Zhang MJ, Huo LJ, Xu F, Wu Y, Hou JH (2012) Design, synthesis and photovoltaic properties of a new D-pi-A polymer with extended pi-bridge units. J Mater Chem 22:21024–21031
135. Zhang SQ, Ye L, Wang Q, Li ZJ, Guo X, Huo LJ, Fan HL, Hou JH (2013) Enhanced photovoltaic performance of diketopyrrolopyrrole (DPP)-based polymers with extended pi conjugation. J Phys Chem C 117:9550–9557
136. Qian DP, Ye L, Zhang MJ, Liang YR, Li LJ, Huang Y, Guo X, Zhang SQ, Tan ZA, Hou JH (2012) Design, application, and morphology study of a new photovoltaic polymer with strong aggregation in solution state. Macromolecules 45:9611–9617
137. Wang M, Hu XW, Liu P, Li W, Gong X, Huang F, Cao Y (2011) Donor acceptor conjugated polymer based on naphtho[1,2-c:5,6-c]bis[1, 2, 5]thiadiazole for high-performance polymer solar cells. J Am Chem Soc 133:9638–9641
138. Huo LJ, Guo X, Zhang SQ, Li YF, Hou JH (2011) PBDTTTZ: a broad band gap conjugated polymer with high photovoltaic performance in polymer solar cells. Macromolecules 44:4035–4037

139. Zhang MJ, Gu Y, Guo X, Liu F, Zhang SQ, Huo LJ, Russell TP, Hou JH (2013) Efficient polymer solar cells based on benzothiadiazole and alkylphenyl substituted benzodithiophene with a power conversion efficiency over 8 %. Adv Mater 25:4944–4949
140. Zhang M, Guo X, Zhang S, Hou J (2014) Synergistic effect of fluorination on molecular energy level modulation in highly efficient photovoltaic polymers. Adv Mater 26:1118–1123
141. Huo LJ, Ye L, Wu Y, Li ZJ, Guo X, Zhang MJ, Zhang SQ, Hou JH (2012) Conjugated and nonconjugated substitution effect on photovoltaic properties of benzodifuran-based photovoltaic polymers. Macromolecules 45:6923–6929
142. Wu Y, Li ZJ, Guo X, Fan HL, Huo LJ, Hou JH (2012) Synthesis and application of dithieno [2,3-d:2′,3′-d′]benzo[1,2-b:4,5-b′] dithiophene in conjugated polymer. J Mater Chem 22:21362–21365
143. Wu Y, Li ZJ, Ma W, Huang Y, Huo LJ, Guo X, Zhang MJ, Ade H, Hou JH (2013) PDT-S-T: a new polymer with optimized molecular conformation for controlled aggregation and pi-pi stacking and its application in efficient photovoltaic devices. Adv Mater 25:3449–3455
144. Son HJ, Lu LY, Chen W, Xu T, Zheng TY, Carsten B, Strzalka J, Darling SB, Chen LX, Yu LP (2013) Synthesis and photovoltaic effect in dithieno[2,3-d:2′,3′-d′]Benzo[1,2-b:4,5-b′] dithiophene-based conjugated polymers. Adv Mater 25:838–843
145. Pron A, Berrouard P, Leclerc M (2013) Thieno[3,4-c]pyrrole-4,6-dione-based polymers for optoelectronic applications. Macromol Chem Physic 214:7–16
146. Zou YP, Najari A, Berrouard P, Beaupre S, Aich BR, Tao Y, Leclerc M (2010) A thieno[3,4-c] pyrrole-4,6-dione-based copolymer for efficient solar cells. J Am Chem Soc 132:5330–5331
147. Zhang Y, Hau SK, Yip HL, Sun Y, Acton O, Jen AKY (2010) Efficient polymer solar cells based on the copolymers of benzodithiophene and thienopyrroledione. Chem Mater 22:2696–2698
148. Zhang GB, Fu YY, Zhang Q, Xie ZY (2010) Benzo[1,2-b:4,5-b′]dithiophene-dioxopyrrolothiophen copolymers for high performance solar cells. Chem Commun 46:4997–4999
149. Piliego C, Holcombe TW, Douglas JD, Woo CH, Beaujuge PM, Frechet JMJ (2010) Synthetic control of structural order in N-alkylthieno[3,4-c]pyrrole-4,6-dione-based polymers for efficient solar cells. J Am Chem Soc 132:7595–7597
150. Aich BR, Lu JP, Beaupre S, Leclerc M, Tao Y (2012) Control of the active layer nanomorphology by using co-additives towards high-performance bulk heterojunction solar cells. Org Electron 13:1736–1741
151. Cabanetos C, El Labban A, Bartelt JA, Douglas JD, Mateker WR, Frechet JMJ, McGehee MD, Beaujuge PM (2013) Linear side chains in benzo[1,2-b:4,5-b′]dithiophene-thieno[3,4-c] pyrrole-4,6-dione polymers direct self-assembly and solar cell performance. J Am Chem Soc 135:4656–4659
152. Amb CM, Chen S, Graham KR, Subbiah J, Small CE, So F, Reynolds JR (2011) Dithienogermole as a fused electron donor in bulk heterojunction solar cells. J Am Chem Soc 133:10062–10065
153. Small CE, Chen S, Subbiah J, Amb CM, Tsang SW, Lai TH, Reynolds JR, So F (2012) High-efficiency inverted dithienogermole-thienopyrrolodione-based polymer solar cells. Nat Photonics 6:115–120
154. Zhong HL, Li Z, Deledalle F, Fregoso EC, Shahid M, Fei ZP, Nielsen CB, Yaacobi-Gross N, Rossbauer S, Anthopoulos TD, Durrant JR, Heeney M (2013) Fused dithienogermolodithiophene low band gap polymers for high-performance organic solar cells without processing additives. J Am Chem Soc 135:2040–2043
155. Su MS, Kuo CY, Yuan MC, Jeng US, Su CJ, Wei KH (2011) Improving device efficiency of polymer/fullerene bulk heterojunction solar cells through enhanced crystallinity and reduced grain boundaries induced by solvent additives. Adv Mater 23:3315–3319
156. Guo XG, Ortiz RP, Zheng Y, Kim MG, Zhang SM, Hu Y, Lu G, Facchetti A, Marks TJ (2011) Thieno[3,4-c]pyrrole-4,6-dione-based polymer semiconductors: toward high-performance, air-stable organic thin-film transistors. J Am Chem Soc 133:13685–13697

157. Guo XG, Zhou NJ, Lou SJ, Smith J, Tice DB, Hennek JW, Ortiz RP, Navarrete JTL, Li SY, Strzalka J, Chen LX, Chang RPH, Facchetti A, Marks TJ (2013) Polymer solar cells with enhanced fill factors. Nat Photonics 7:825–833
158. Wang EG, Hou LT, Wang ZQ, Hellstrom S, Zhang FL, Inganas O, Andersson MR (2010) An easily synthesized blue polymer for high-performance polymer solar cells. Adv Mater 22:5240–5244
159. Wang EG, Ma ZF, Zhang Z, Vandewal K, Henriksson P, Inganas O, Zhang FL, Andersson MR (2011) An easily accessible isoindigo-based polymer for high-performance polymer solar cells. J Am Chem Soc 133:14244–14247
160. Qian DP, Ma W, Li ZJ, Guo X, Zhang SQ, Ye L, Ade H, Tan ZA, Hou JH (2013) Molecular design toward efficient polymer solar cells with high polymer content. J Am Chem Soc 135:8464–8467
161. Deng Y, Liu J, Wang J, Liu L, Li W, Tian H, Zhang X, Xie Z, Geng Y, Wang F (2014) Dithienocarbazole and isoindigo based amorphous low bandgap conjugated polymers for efficient polymer solar cells. Adv Mater 26:471–476
162. Osaka I, Kakara T, Takemura N, Koganezawa T, Takimiya K (2013) Naphthodithiophene-naphthobisthiadiazole copolymers for solar cells: alkylation drives the polymer backbone flat and promotes efficiency. J Am Chem Soc 135:8834–8837
163. Hendriks KH, Heintges GHL, Gevaerts VS, Wienk MM, Janssen RAJ (2013) High-molecular-weight regular alternating diketopyrrolopyrrole-based terpolymers for efficient organic solar cells. Angew Chem Int Ed 52:8341–8344
164. Dou L, Chen C-C, Yoshimura K, Ohya K, Chang W-H, Gao J, Liu Y, Richard E, Yang Y (2013) Synthesis of 5H-dithieno[3,2-b:2′,3′-d]pyran as an electron-rich building block for donor–acceptor type low-bandgap polymers. Macromolecules 46:3384–3390
165. Ye L, Zhang SQ, Qian DP, Wang Q, Hou JH (2013) Application of Bis-PCBM in polymer solar cells with improved voltage. J Phys Chem C 117:25360–25366
166. Zhang X, Lu Z, Ye L, Zhan C, Hou J, Zhang S, Jiang B, Zhao Y, Huang J, Zhang S, Liu Y, Shi Q, Liu Y, Yao J (2013) A potential perylene diimide dimer-based acceptor material for highly efficient solution-processed non-fullerene organic solar cells with 4.03 % efficiency. Adv Mater 25:5791–5797
167. Jiang W, Ye L, Li XG, Xiao CY, Tan F, Zhao WC, Hou JH, Wang ZH (2014) Bay-linked perylene bisimides as promising non-fullerene acceptors for organic solar cells. Chem Commun 50:1024–1026
168. Sonar P, Lim JPF, Chan KL (2011) Organic non-fullerene acceptors for organic photovoltaics. Energy Environ Sci 4:1558–1574
169. Eftaiha AF, Sun JP, Hill IG, Welch GC (2014) Recent advances of non-fullerene, small molecular acceptors for solution processed bulk heterojunction solar cells. J Mater Chem A 2:1201–1213
170. Facchetti A (2013) Polymer donor-polymer acceptor (all-polymer) solar cells. Mater Today 16:123–132
171. Zhan XW, Tan ZA, Domercq B, An ZS, Zhang X, Barlow S, Li YF, Zhu DB, Kippelen B, Marder SR (2007) A high-mobility electron-transport polymer with broad absorption and its use in field-effect transistors and all-polymer solar cells. J Am Chem Soc 129:7246–7247
172. Zhan XW, Tan ZA, Zhou EJ, Li YF, Misra R, Grant A, Domercq B, Zhang XH, An ZS, Zhang X, Barlow S, Kippelen B, Marder SR (2009) Copolymers of perylene diimide with dithienothiophene and dithienopyrrole as electron-transport materials for all-polymer solar cells and field-effect transistors. J Mater Chem 19:5794–5803
173. Tan ZA, Zhou EJ, Zhan XW, Wang X, Li YF, Barlow S, Marder SR (2008) Efficient all-polymer solar cells based on blend of tris(thienylenevinylene)-substituted polythiophene and poly[perylene diimide-alt-bis(dithienothiophene)]. Appl Phys Lett 93:073309
174. Zhou EJ, Cong JZ, Wei QS, Tajima K, Yang CH, Hashimoto K (2011) All-polymer solar cells from perylene diimide based copolymers: material design and phase separation control. Angew Chem Int Ed 50:2799–2803

175. Zhou Y, Yan QF, Zheng YQ, Wang JY, Zhao DH, Pei J (2013) New polymer acceptors for organic solar cells: the effect of regio-regularity and device configuration. J Mater Chem A 1:6609–6613
176. McNeill CR, Abrusci A, Zaumseil J, Wilson R, McKiernan MJ, Burroughes JH, Halls JJM, Greenham NC, Friend RH (2007) Dual electron donor/electron acceptor character of a conjugated polymer in efficient photovoltaic diodes. Appl Phys Lett 90:193506
177. McNeill CR, Abrusci A, Hwang I, Ruderer MA, Muller-Buschbaum P, Greenham NC (2009) Photophysics and photocurrent generation in polythiophene/polyfluorene copolymer blends. Adv Funct Mater 19:3103–3111
178. Tang YQ, McNeill CR (2013) All-polymer solar cells utilizing low band gap polymers as donor and acceptor. J Polym Sci B: Polym Phys 51:403–409
179. Earmme T, Hwang YJ, Murari NM, Subramaniyan S, Jenekhe SA (2013) All-polymer solar cells with 3.3 % efficiency based on naphthalene diimide-selenophene copolymer acceptor. J Am Chem Soc 135:14960–14963
180. Cheng P, Ye L, Zhao X, Hou J, Li Y, Zhan X (2014) Binary additives synergistically boost the efficiency of all-polymer solar cells up to 3.45 %. Energy Environ Sci. doi:10.1039/C3EE43041C
181. Zhou E, Cong JZ, Hashimoto K, Tajima K (2013) Control of miscibility and aggregation via the material design and coating process for high-performance polymer blend solar cells. Adv Mater 25:6991–6996
182. Mori D, Benten H, Okada I, Ohkita H, Ito S (2013) Low-bandgap donor/acceptor polymer blend solar cells with efficiency exceeding 4 %. Adv Energy Mater. doi:10.1002/aenm.201301006
183. Chiechi RC, Hummelen JC (2012) Polymer electronics, quo vadis? Acs Macro Lett 1:1180–1183
184. Koster LJA, Shaheen SE, Hummelen JC (2012) Pathways to a new efficiency regime for organic solar cells. Adv Energy Mater 2:1246–1253
185. Kanal IY, Owens SG, Bechtel JS, Hutchison GR (2013) Efficient computational screening of organic polymer photovoltaics. J Phys Chem Lett 4:1613–1623
186. Liu C, Wang K, Hu XW, Yang YL, Hsu CH, Zhang W, Xiao S, Gong X, Cao Y (2013) Molecular weight effect on the efficiency of polymer solar cells. ACS Appl Mater Inter 5:12163–12167